



**NTNU – Trondheim**  
Norwegian University of  
Science and Technology

# Study of the Droplet-Interface Dynamics Related to Liquid-Liquid Separators

**Marthin Sveier**

Master of Energy and Environmental Engineering

Submission date: June 2012

Supervisor: Carlos Alberto Dorao, EPT

Norwegian University of Science and Technology  
Department of Energy and Process Engineering



EPT-M-2012-82

**MASTER THESIS**Marthin Sveier  
Stud.techn.  
Spring 2012*Study of the droplet-interface dynamic related to liquid-liquid separators*  
**Studier av dråpe-interfase dynamikk i væske-væske separasjon**

Liquid-liquid separators are integral part of many industrial processes. Water entrained in oil and other hydrocarbon products can impede quality specifications. The equipment used for bulk separation operations in offshore activities to produce oil and gas is of considerable size and weight. A critical parameter for the sizing of separators is related to the dynamic of the droplet interacting with the liquid-liquid interface.

In this work the coalescence time of droplets interacting with the liquid-liquid interface will be study. The study will investigate the dependency of the droplet size in the coalescence time.

**The following tasks are to be considered:**

1. Review the models for predicting droplet-interface coalescence time, and droplet settling velocity
2. Construct the test unit, and calibration of the visualization system.
3. Construct the micro-size droplet generation
4. Perform a detail error analysis and comparison of the results with the available data

-- " --

Within 14 days of receiving the written text on the master thesis, the candidate shall submit a research plan for his project to the department.

When the thesis is evaluated, emphasis is put on processing of the results, and that they are presented in tabular and/or graphic form in a clear manner, and that they are analyzed carefully.

The thesis should be formulated as a research report with summary both in English and Norwegian, conclusion, literature references, table of contents etc. During the preparation of the text, the candidate should make an effort to produce a well-structured and easily readable report. In order to ease the evaluation of the thesis, it is important that the cross-references are correct. In the making of the report, strong emphasis should be placed on both a thorough discussion of the results and an orderly presentation.

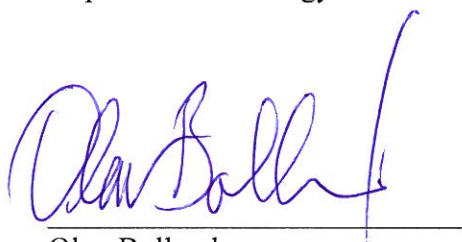
The candidate is requested to initiate and keep close contact with his/her academic supervisor(s) throughout the working period. The candidate must follow the rules and regulations of NTNU as well as passive directions given by the Department of Energy and Process Engineering.

Risk assessment of the candidate's work shall be carried out according to the department's procedures. The risk assessment must be documented and included as part of the final report. Events related to the candidate's work adversely affecting the health, safety or security, must be documented and included as part of the final report.

Pursuant to "Regulations concerning the supplementary provisions to the technology study program/Master of Science" at NTNU §20, the Department reserves the permission to utilize all the results and data for teaching and research purposes as well as in future publications.

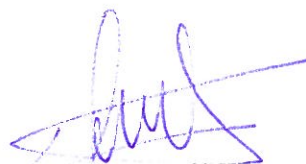
The final report is to be submitted digitally in DAIM. An executive summary of the thesis including title, student's name, supervisor's name, year, department name, and NTNU's logo and name, shall be submitted to the department as a separate pdf file. Based on an agreement with the supervisor, the final report and other material and documents may be given to the supervisor in digital format.

Department of Energy and Process Engineering, 30. January 2012



---

Olav Bolland  
Department Head



---

Carlos A. Doraó  
Academic Supervisor

# Preface

This report is my conclusion of my Energy and Environmental Engineering Master program at the Norwegian University of Science and Technology. Moreover, it is also a conclusion of my stay at the Department of Energy and Process Engineering and the Natural Gas Technology Group.

I would like to direct my thanks to my supervisor, Prof. Carlos A. Dorao for helping and guiding me through both project- and master thesis. He gave me a lot of freedom and responsibility on this project. The inputs he gave, spread way beyond simple guidance and I am thankful to have learned this much. His commitment during the very hectic ending of the project is not forgotten.

Moreover, big thanks are directed to Nicolas La Forgia, soon to be P.hD., while being busy with his own project, he always found time to help. His knowledge and know-how about optics, electronics and software have been invaluable to me.

In addition, I am grateful to all those who, with their help and support, made this thesis possible. In particular, my parents who have motivated and supported me through these five years of studies in multiple countries. Their encouragement has meant a lot to me. Last, I would like to thank all the people I have met and the friends I have made during this time, thank you for making this such a happy period of my life, I hope to see you all again.

## Abstract

A widespread use of liquid liquid separators are taking place in many industrial processes, especially in production of hydrocarbons. The separators in oil production are used to separate water from oil, increasing the purity of petroleum and making cleaner produced water in order to meet quality and environmental standards. To improve the performance of the separators it is important to understand the complex dynamics taking place. The scope of this work has been to develop and build a facility for accurately studying coalescence and coalescence time which is a key parameter in separator dimensioning, the facility is designed for droplets ranging from  $50 \mu m$  to  $1000 \mu m$ . The relationship of droplet size and coalescence time is especially interesting. Theory on droplet formation, behavior and coalescence mechanism are introduced and a special focus is put on generation of the smallest droplets.

Earlier work in this field of study is presented in the background and literature study part. It covers a brief introduction to separator design, coalescence modeling by using basic principles as gravity and surface tension and generation of small droplets by deforming a meniscus with electrostatic forces.

The facility has been developed by step-wise treating obstacles and requirements. Facility development is organized by the various parts and includes droplet generation, illumination, visualization and automation of the experiments. Unfortunately a high voltage amplifier malfunctioned due to a factory error and the generation of the smallest droplets was not demonstrated. The facility is successfully build and can generate, visualize and capture the coalescence for large droplets and is ready to accept smaller ones when the high voltage amplifier is repaired.

While major parts of the facility is completed there is potential for improvement by further work. Besides from demonstrating the generation of the smallest droplets it should be aimed to complete the automation of the facility and to complete the post processing by deciding a decision criteria for coalescence time. In this way a fully automated facility producing and recording hundreds of droplets of a given size can be made, making it possible to do statistical evaluation of the relationship of droplet size and coalescence time.

## Sammendrag

En utstrakt bruk av væske væske separatore er vanlig i mange industrielle prosesser, dette gjelder spesielt i produksjon av hydrokarboner. Separatore i oljeproduksjon brukes til å separere olje fra vann for å øke renheten i både oljen og produsert vann. Dette må gjøres for å imøtekomme kvalitets og miljøkrav. For å forbedre ytelsen til slike separatore er det viktig å forstå den komplekse dynamikken som tar sted. Målet for denne oppgaven har vært å utvikle og bygge en forsøksrigg som kan studere dråpe interfase koalesens og koalesens tid som er en viktig parameter i separator dimensjonering. Forsøksriggen er utviklet for å produsere og teste dråper i størrelsesordenen  $50 \mu m$  til  $1000 \mu m$  hvor forholdet mellom dråpestørrelse og koalesens tid er spesielt interessant. Teori på dråpe formasjon, oppførsel og koalesens mekanismer er introdusert og et spesielt fokus er satt på generering av de minste dråpene.

Tidligere arbeid på dette feltet er presenter i bakgrunds og litteraturstudie seksjonene. De dekker en introduksjon av separator design og koalesens modellering ved å bruke prinsipper som gravitasjon og overflatespenning, i tillegg er generering av små dråper ved å deformere en menisk ved elektrostatiske krefter presentert.

Forsøksriggen har blitt utviklet ved å møte hindringer og utfordringer stegvis. Utviklingen er organisert ved de ulike delene og inkluderer dråpe generering, belysning, visualisering og automatisasjon av eksperimentene. Desverre virket ikke en spenningsforsterker som brukes til å generere de minste dråpene på grunn av en fabrikkfeil, demonstrasjon og påvisning av disse dråpene ble dermed ikke gjennomført. Monteringen av forsøksriggen var vellykket og kan generere, visualisere og fange koalesens for store dråper og er klar til å ta i mot de minste dråpene når spenningsforsterkeren er reparert.

Forsøksriggen er i operativ stand og store deler av den er ferdig, men fortsatt er det rom for fremtidige forbedringer. Bortsett fra å demonstrere generering av de minste dråpene bør automatisasjonen av riggen fullføres, dette inkluderer også å finne et beslutningskriterie for koalesens som kan brukes i posesseringen av data. På denne måten kan en fullt automatisert rigg produsere hundrevis av dråper for hver eneste dråpestørrelse og gjøre det mulig å gjennomføre en skikkelig og nøyaktig statistisk evaluering av forholdet mellom dråpestørrelse og koalesens tid.





# Contents

<b>List of symbols</b>	<b>iii</b>
<b>1 Introduction</b>	<b>1</b>
1.1 Background . . . . .	2
1.2 Objective and Scope of the Work . . . . .	6
1.3 Report Structure . . . . .	6
<b>2 Literature Study and Theoretical Overview</b>	<b>7</b>
2.1 Droplet Surface Coalescence . . . . .	11
2.1.1 Film Formation . . . . .	12
2.1.2 Film Draining and Rupture . . . . .	12
2.2 Droplet Breakup . . . . .	15
2.2.1 Kelvin-Helmholtz and Rayleigh-Taylor Instabilities . . . . .	15
2.2.2 Shear Stresses . . . . .	16
2.2.3 Surfactants . . . . .	17
2.3 Terminal Velocity . . . . .	18
2.4 Micro Size Droplets Generation . . . . .	19
2.4.1 Multi-Stage Pulse . . . . .	22
<b>3 Requirements and Specification for the Design of the Experimental Facility</b>	<b>25</b>
<b>4 Results and Discussion</b>	<b>27</b>
4.1 Micro Droplet Generation . . . . .	27
4.2 Droplet Detection . . . . .	28
4.3 Illumination . . . . .	30
4.3.1 Absorption Spectroscopy . . . . .	32
4.4 Visualization . . . . .	34
4.5 High Speed Visualization . . . . .	38
4.5.1 Experimental Considerations . . . . .	40
4.5.2 Image Calibration . . . . .	41
4.6 Data Acquisition Chain and Automation . . . . .	46
4.6.1 Post Processing . . . . .	49

4.6.2	Drop Size Measurement . . . . .	51
4.7	Facility . . . . .	52
<b>5</b>	<b>Conclusion and Recommendation</b>	<b>55</b>
5.1	Conclusion . . . . .	55
5.2	Recommendation . . . . .	56
<b>A</b>	<b>'getAllFiles'</b>	<b>62</b>
<b>B</b>	<b>'removeThumbs'</b>	<b>63</b>
<b>C</b>	<b>'imgProc'</b>	<b>64</b>

# List of symbols

<i>symbol</i>	<i>description</i>	<i>units</i>
$F_D$	drag force	[N]
$F_g$	gravitational force	[N]
$d, \emptyset$	diameter	[m]
$r, R$	radius	[m]
$h_{in}$	initial film hight	[m]
$h_c$	critical film hight	[m]
$R_c$	projected radius	[m]
$V_t$	terminal settling velocity	[m/s]
$U$	bulk velocity	[m/s]
$V_d$	draining velocity	[m/s]
$V_{Re}$	Reynolds thinning velocity	[m/s]
$v$	hole expansion velocity	[m/s]
$P_0, P_{cap}$	capillary pressure	[Pa]
$\Delta p$	pressure difference	[Pa]
$\Delta \rho$	density difference	[kg/m <sup>3</sup> ]
$A_H$	Hamaker constant	[-]
$\prod_{el}$	electrostatic repulsion	[-]
$\prod_w$	Van der Waals	[-]
$We$	Weber number	[-]
$We^*$	modified Weber number	[-]
$Re$	Reynolds number	[-]
$Ca$	capillary number	[-]
$g$	gravity	[m/s <sup>2</sup> ]
fps	frames per second	[frames/s]
$E$	electric field	[V/m]
$\epsilon$	permittivity	[-]
$L$	length	[m]
$t$	time	[s]
<i>Greek symbols</i>		
$\eta, \mu$	dynamic viscosity	[Pa · s]
$\rho$	density	[kg/m <sup>3</sup> ]
$\tau$	coalescence time	[s]

$\sigma$	interface tension	[kg/m <sup>3</sup> ]
<i>subscripts</i>		
s	drop	
f	film	
L	lead	
P	pulse	
T	trail	
a	major axis	
b	minor axis	
cap	capillary	

# Chapter 1

## Introduction

Liquid-liquid separators are integral parts of many industrial processes, the oil and gas industry in particular. Water dispersed in oil and other hydrocarbon products can result in failure of reaching quality specifications. Separators are used to extract the different phases in order to meet quality, safety and environmental demands. Their importance effectively lead to a wide spread use of separators that are of considerable size and weight. These features could be problematic as separators are often used in locations where there are constrains on space and weight or there are considerable economical penalties on the demand of such. Prime examples of locations where this could be a issue are in subsea installations and on offshore platforms. A key parameter in separator dimensioning is related to the dynamics of droplets interacting with the liquid-liquid interface. The time it takes from a droplet has merged or coalesced with its interface is named coalescence time and is effectively dimensioning the separator. By improving the understanding of the dynamics, measures can be taken to reduce the coalescence time. Currently a combination of additive agents, electrostatic coalescence and large vessels are used to find the best fit between cost and quality.

To illustrate the extent of liquid-liquid separation, the production of oil on the Norwegian continental shelf was about 104 million  $\text{Sm}^3$  in 2010 [SSB, 2010]. The Norwegian production is only a fraction on the global scale and a small player compared to the really big nations like Russia, Saudi Arabia and the Arab League. As the amount of large- easy accessible and producible sources of hydrocarbons are running out, the exploitation of mature and previous discovered marginal fields becomes important. Likewise are sources under difficult and extreme conditions like deep-water on the coast of Brazil and in the icy and weathered environment of the Barents sea becoming increasingly more interesting. As the complexity of operations increases, so does the requirement to organizations and equipment. If the performance of separators could be improved it would mean major savings in space or improved production capacity, which would be very beneficial in obtaining a stable and solid production, critical for risk management.

## 1.1 Background

To obtain a better understanding of separation as a process and the challenges with it, a simple horizontal separator for two-phase flow will be introduced. The aim is to briefly explain the different steps of separation and measures to meet the challenges, not to design a separator.

The basic principles of gravity settling and coalescence will be the main focus, but separators also make use of momentum force in order to separate phases and solids. An example of momentum force application is bulk separation of gas, liquids and solids directly from a well. The incoming flow is met by a diverter that changes the direction of the flow and efficiently separates gas from liquids and solids. This sudden change of flow direction and utilization of momentum force are mixing oil with water, a common way to treat this mixture is by water washing. The mixture is directed through a column of water, washing out a large fraction of water from the mixture. The product after water washing is termed emulsion, that is a mixture of two or more liquids which are normally immiscible (unblendable). In an emulsion, one liquid phase is dispersed in the other continuous liquid phase. Now, the velocity should be low and gravitational force is allowed to work on the two fluids and droplets of oil and water are settling out. Accordingly, a layer of oil will form on the top of the emulsion and water will settle to the bottom. If given enough time more or less all of the oil and water droplets will be separated by gravity and join their homophase which could be hour, days or even months. The smallest droplets are so small that they are not substantially affected by the gravity force, examples are mist in gas or dispersed oil and water droplets. Coalescence as the third concept of separation are then coming into play. By merging small droplets together by coalescence, the gravity force can act on the new droplet and hence drastically reduce the separation time. Most gravity separators make use of the same kind of components and features [ Mokhatab, 2006].

- A primary gas/liquid separation section with an inlet diverter to remove the bulk of the liquid from the gas.
- A gravity-settling section providing adequate retention time so that proper settling may take place.
- A mist extractor at the gas outlet to capture entrained droplets or those too small to settle by gravity.
- Proper pressure and liquid-level controls.

A two phase separator is specialized in separating oil and water and is fairly normal downstream from initial treatment. The fluid entering the separator will have a jet-like shape and hence turbulence are generated when the jet is broken down, for this reason a turbulence plate is added. Further a dedicated coalescence unit is added that works with a settling unit in order to enhance gravity settling. After the fluid is treated in these two

units it will be subjected to gravity forces and the phases are separated before they are pumped out.

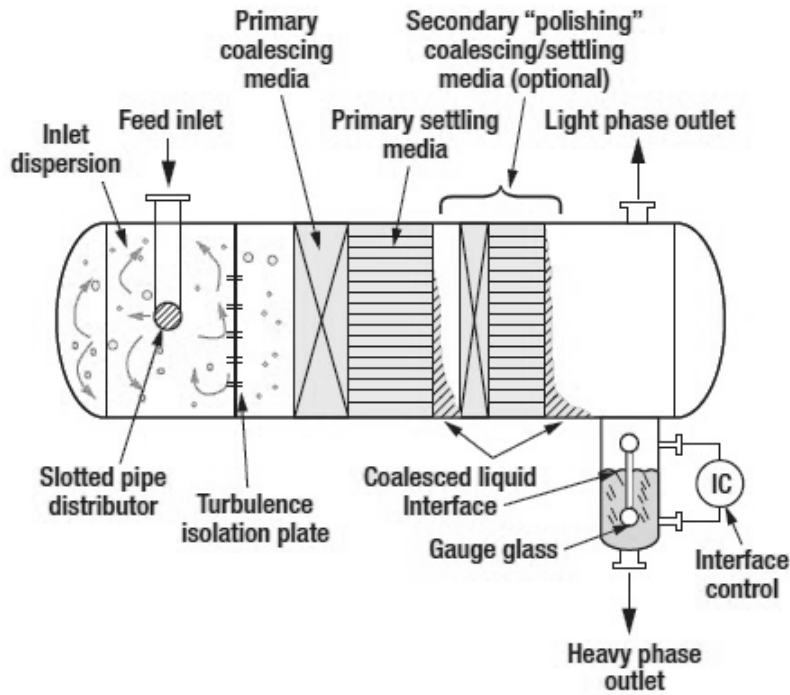


Figure 1.1: *Schematics of a two-phase separator with added coalescence and settling units [Cusack, 2009]*

It is worth noticing that the primary settling medium consist of channels where the separating of water and oil takes place. The benefit of using channels instead of a big chamber are many [Cusack, 2009]:

- Decreases the effective diameter, thereby greatly reduce the Reynolds number of the flowing fluid and producing a deep laminar flow environment that enhances the gravity settling rate.
- Isolates the fluid in separate channels, thereby putting limits on how far droplets can "wander" and reducing the negative impact of eddy currents.
- Decrease the distance a droplet needs to rise or fall before reaching an interface, thereby greatly lowering settling time requirement.
- Provide multiple interfaces inside the equipment where droplets can coalesce, thereby greatly increasing the coalescence process.

Targets are inserted in the flow path, the droplets impacts and are collected on the surface of the targets due to surface energy forces. When collected the droplets coalesce to form larger droplets that are more prone to gravity forces. A typical corrugated plate packing used for this purpose can be seen in figure 1.2.

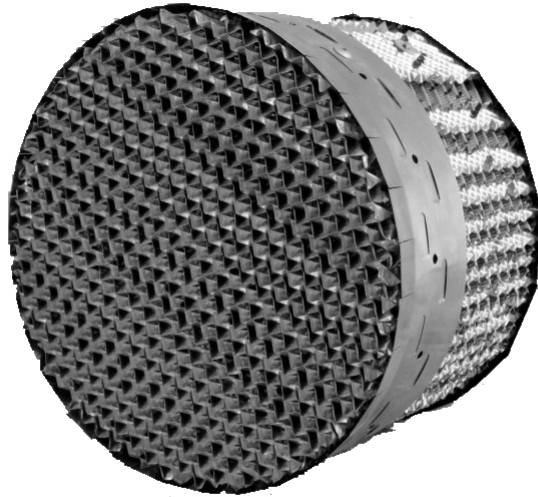


Figure 1.2: *A corrugated plate packing give droplets a very high collecting surface area*

By narrowing channels, tiny droplet are merged and the effect of gravity forces becomes bigger. A drawback of such units is the risk of fouling due to sand, paraffins and corrosion from other parts of the system.

The ultimate goal for this project is to facilitate study of coalescence time dependent on droplet size, based on the retrieved information by such studies, coalescence of droplets on a flat interface can be better understood. Similar studies based on droplets in the size of millimeters were performed as early as in the 1960's by [Charles and Mason, 1960] and by [Gillespie and Rideal, 1956] with the conclusion that coalescence time increase with size in this range. Later, [Langl and Wilke, 1971] found that sonic disturbances could lead to the opposite trend with decreased coalescence time relative to size, similar findings were found in the preliminary studies, but no clear connection to external factors as sound was identified. The results from these studies are plotted in figure 1.3, except by the one from [Langl and Wilke, 1971] due to lack of data.



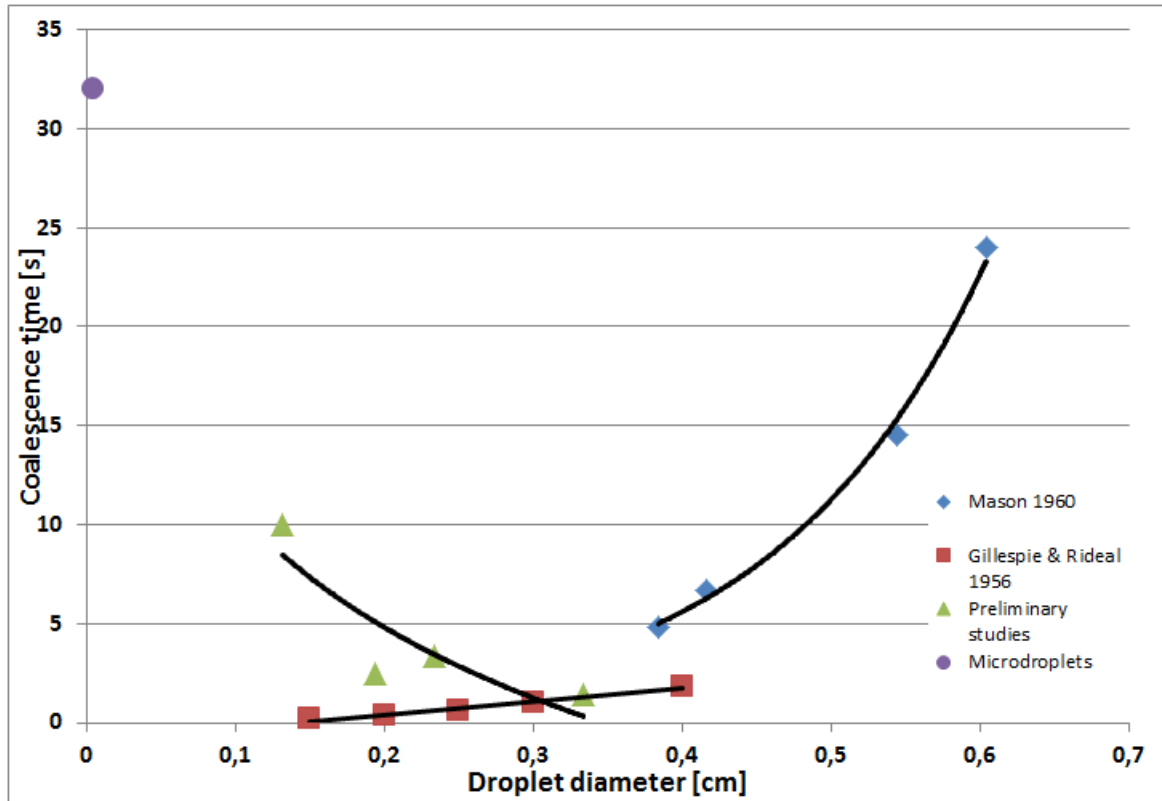


Figure 1.3: *Coalescence time based on droplet size, tilted squares - Charles Mason 1960 with 50 samples per size, horizontal squares - Gillespie and Rideal, 1956 with 100 samples and the triangles from the preliminary studies with 25 samples per size. In addition, coalescence time for micro size droplets are indicated by a single circle to illustrate that coalescence time is expected to increase dramatically*

A Benzene/Water system is utilized by the two published studies while a Exxsol D80/Water system is used in the preliminary studies. All the systems are at 20 °C which allows the Benzene/Water systems to be compared directly. The main point of attention should be the trend lines of the two, indicating increasing coalescence time with size being the established truth. We know for a fact that tiny microdroplets use a very long time for coalescing, but no studies are found that investigate droplets in this range mainly due to lack of successfully produce homogeneous droplets. The result of completing a study with both micro- and millimeter size droplets could be a U-shaped coalescence profile based on size. Alternatively, the profile could contain local and highly interesting maxima and minima. The coalescence and dependence of the droplet size is a critical parameter in predicting separator efficiency. This study aims to facilitate further detailed investigation in both known and partially unknown scale of droplet-magnitude

## 1.2 Objective and Scope of the Work

The development of a facility for investigating droplet - interface coalescence is essential to perform detailed and reliable investigations on the relationship between coalescence and droplet size. The main goals were to design and construct a visualization unit which could be used in droplet - interface experiments and allow the production of micro size droplets. The challenge is to produce a set of homogeneous droplets with consistent shape and size. It is possible to make micro size droplets by trial and error, but it is a demand of very high droplet reproducibility to do a statistical evaluation. Conditions have to be near identical which means that droplet shape and size are to be constant and that no disturbing trail, daughter or "cloud" of droplets often made by sprays are present. To meet all these criteria by manual operation is near impossible and a micro size droplet systems must be constructed. Experiments were performed for testing the facility and deciding on how to make the best results. It has been important to test and find the best composition of liquids, optimal light source, most accurate triggering of camera - light interaction, and optimal parameters for visualization. They are all essential aspects in analyzing droplet - interface experiments and their testing have given useful information and conclusions.

This project will limit to study coalescence at a pure droplet - interface system, coalescence enhancers like additives and electro coalescence are not tested, neither is droplet - droplet coalescence. The liquids in play are confined to two samples of heavy and light petroleum, the transparent oil Exxsol D80 and water. The suitability of Exxsol D80 has proven itself in a numerous of studies while systems of petroleum and water are tested. Finally the facility is designed for droplets with diameter of millimeters to micrometers.

## 1.3 Report Structure

Chapter 2 presents theory on droplet interface coalescence describing the droplet behavior, film formation, draining, rupture, coalescence time and terminal velocity. An extensive study of literature is made and presented in table 2.1. The requirements and specification for the design of the experimental facility is presented in chapter 3 and efficiently sums up the restrictions of the facility on setup size, droplet size range, image quality, liquids and more.

Chapter 5, the Results and Discussion chapter gives a very thorough walk trough of the facility assumptions and development. The chapter aims to give the reader a better understanding of the challenges met and the amount of work required to develop the facility. It is organized by the respective sub units and covers topics like micro size droplet generation, droplet detection, visualization and automation.

Finally is the Conclusion and Recommendation giving conclusions on the performance of the developed facility and recommendation for further work in improving it. Appendix A, B and C contains the developed MATLAB codes used for processing.

## Chapter 2

# Literature Study and Theoretical Overview

The description of coalescence and break up mechanisms of fluid particles at an interface or in a continuum fluid is very important in many industrial processes. The efficiency of mixing vessels and separators are highly dependent on these mechanism, making the description essential to predict the performance of such systems. Different mathematical separation models for a liquid-liquid interface have been developed. The models can roughly be divided into two groups, the deterministic models focus on the drainage of a thin layer between drop and interface while the probability models consider the separation to be a stochastic process. The complex interaction of various influencing effects make the coalescence in a gravity settler seem to be a stochastic process, because there are little knowledge about fundamental effects and principles of chemistry and colloid science. As a first step to the theoretical calculation of settlers the coalescence of a single droplet at a planar interface is studied.

The concept of surface tension is making it possible for discrete fluid particles to be present in a continuum fluid. It is observed, when a liquid is poured onto a solid surface that it tends to form in droplet shaped bodies instead of spreading out even on the whole surface. To clearer understand this behavior the organizing of molecules within a liquid is shown in figure 2.1.

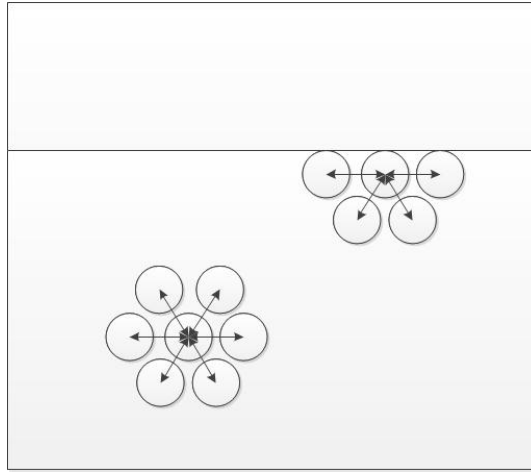


Figure 2.1: A molecule that is located within the liquid are acting upon molecules that are surrounding it, while a molecule that is located at the surface is only acting with other molecules beneath and on it's sides

This uneven distribution of forces is effectively pulling the surface molecules toward the center of the liquid. This positioning of molecules is at it most stable when the surface area is reduced to its minimum, shaped like a spherical droplet. Surface tension is the result from forces between molecules - intermolecular forces, the coalescence and break up of droplets is essentially about overcoming these forces. A table of literature with author and topic details are given below to give a better overview of the theory used in this work.

Table 2.1: An overview of literature used and the topics of the work

Author	Title of work	Key words
Basheva, 1999	Size Dependence of the Stability of Emulsion Drops Pressed against a Large Interface	Rule of thumb for distance of drop-interface interaction, Emulsion
Traykov, Ivanov, 1977	Hydrodynamics of thin liquid films.	Film thinning, emulsions, effect of surfactants
O. Reynolds, 1886	On the Theory of Lubrication and Its Application to Mr. Beauchamp Tower's Experiments, Including an Experimental Determination of the Viscosity of Olive Oil	Reynolds classic experiment, film thinning velocity
Charles and Mason, 1960	The coalescence of liquid drops with flat liquid/liquid interfaces	Thinning velocity, coalescence time, droplet on plane surface, film rupture, partial coalescence
Continued on next page		

**Table 2.1 – continued from previous page**

<b>Author</b>	<b>Title of work</b>	<b>Key words</b>
Vrij, 1966	Possible Mechanism for the Spontaneous Rupture of Thin, Free Liquid Films	Film rupture, critical film thickness based on the Hamaker constant
A. Dupre, 1869	Théorie Mécanique de la Chaleu	Estimation of hole expansion velocity
M. Dhainaut, 2002	Literature Study on Observations and Experiments on Coalescence and Breakup of Bubbles and Drops	Droplet breakup, treating K-Helmholtz and Taylor instabilities, effect of surfactant
Janssen, 1993	Droplet breakup mechanisms: Stepwise equilibrium versus transient dispersion	Shear stress, capillary number - droplet breakup
Grace, 1971	Dispersion phenomena in high viscosity immiscible fluid systems and application of static mixers as dispersion devices in such systems	shear stress, critical Capillary number
Taylor, 1934	The Formation of Emulsions in Definable Fields of Flow	Emulsions, critical Capillary number
Stewart, 2008	Gas-Liquid And Liquid-Liquid Separators	Design of two and three phase separators
Mokhatab, 2006	Handbook of Natural Gas Transmission and Processing	Components in a separator
Cusack, 2009	Rethink your liquid-liquid separations	Design of settling medium in separator
Langl and Wilke, 1971	A Hydrodynamic Mechanism for the Coalescence of Liquid Drops. I. Theory on Coalescence at a Planar Interface	Theory on drop-interface coalescence
Langl and Wilke, 1971	A Hydrodynamic Mechanism for the Coalescence of Liquid Drops. II. Experimental Studies	Experimental study of coalescence time, single stage coalescence, sonic/subsonic noise effect on coalescence time
Lawrence, Nielsen and Adams, 1958	Coalescence of liquid drops at oil-water interfaces	Predicts increased coalescence time with size
Pearson, 1916	Mathematical Contributions to the Theory of Evolution. XIX. Second Supplement to a Memoir on Skew Variation	Prediction of statistically distribution, the Pearson diagram
Tsukatan and Shigemitsu, 1980	Simplified Pearson distributions applied to air pollutant concentration	Visualized Pearson groups in a diagram
SSB, 2010	Produksjon og reserver, 4. kvartal 2010	Statistics on Norwegian oil and gas production

Continued on next page

**Table 2.1 – continued from previous page**

<b>Author</b>	<b>Title of work</b>	<b>Key words</b>
Perry, J. H., Ed., 1950	Chemical Engineers Handbook	Characteristics of dispersed particles
Kassim and Longmire , 2004	Drop coalescence through a liquid/liquid interface	Quantify generation and evolution of vorticity by determine the velocity and vorticity fields through coalescence events
Wright et al. 1993	Self-Consistent Modeling of the Electrohydrodynamics of a conductive Meniscus	Demonstrating drop ejection by single pressure pulse
Atten et al. 2008	Drop-on-demand Extraction from a Water Meniscus by a High Field Pulse	Deformation, break up and generation of a single non-charged water droplet in oil, by applying a voltage pulse.
Raisin, 2011	Electrocoalescence in water-in-oil emulsions: towards an efficiency criterion	Homogeneous generation of micro size droplet in a dielectric liquid
Gillespie and Rideal, 1956	The coalescence of drops at an oil-water interface	Droplet experiments, coalescence time increase with size $d=O(\text{mm})$

## 2.1 Droplet Surface Coalescence

In order to explore the coalescence and break up of droplets, a basic principle of a bottle filled with two liquids of different density  $\rho_1$  and  $\rho_2$ , creates a clear interface on the transition from one liquid to another is applied. Experiments are conducted by releasing a droplet in the top or bottom fluid. Due to the surface tension the droplet will approach a spherical shape as long as the fluid column is long enough. Droplets released from the bottom must be of the fluid from the top  $\rho_1$  and vice versa if the droplet is released from the top it needs to be of the bottom fluid  $\rho_2$ . In this way the droplets will coalesce when they reach the interface instead of just stacking up if they were made of a third component. The possibility of stacking is due to contamination but will be discussed in further detail later. In figure 2.2 the general principle of such systems are indicated.

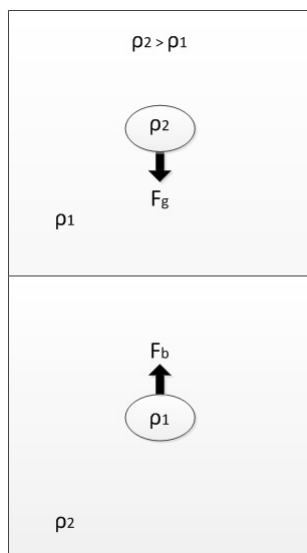


Figure 2.2: *In the top part, a droplet with density  $\rho_2$  is traveling through the segment of  $\rho_1$  driven by the density difference and the gravity. Likewise a droplet with density  $\rho_1$  is traveling through the column of density  $\rho_2$  driven by the density difference and buoyancy*

The two approaches are essentially using the same principles with density difference and gravity as the driving forces, the general case of a droplet released in the top segment will be further discussed with respect to how it approaches the interface and coalescence. A dispersed droplet propagating through the fluid column will continue to accelerate until the counter-current drag force  $F_D$  and gravitational force  $F_g$  in flow direction are balancing each other. The obtained velocity is termed terminal settling velocity  $V_t$  and will be kept constant until the droplet is approaching the interface.

### 2.1.1 Film Formation

As a rule of thumb, the droplet is affected by the presence of an interface at a distance  $d$  - of the droplet diameter, mentioned among others by [Basheva, 1999]. At this point the droplet distinctively decelerates due to the viscous friction with the interface. Assuming that the droplet is incompressible, it will start to deform and create a more or less plane parallel film between the droplet and interface.

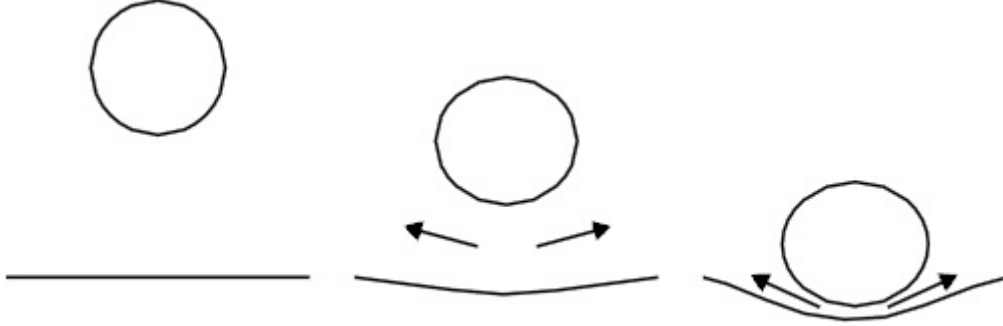


Figure 2.3: *A droplet is progressing through a fluid column, at a distance around one droplet-diameter the presence of an interface is decelerating the droplet. It deforms and a plane parallel film that drains to the sides will start to form*

The film is the origin of  $\tau$  - the coalescence time, which is the time from the droplet arrives to it coalesces with the interface. A second definition of coalescence time is also used that includes the time it takes until the surface has come to rest after the droplet has coalesced. For this approach the time it takes from the droplet has reached the interface and coalescence initiated is called the resting time. Due to the dominant and long timespan of drop resting on the interface it is termed as the coalescence time for the rest of this work. The film draining starts at the initial film height  $h_{in}$  and ends at the critical height  $h_{cr}$ .

$$\tau = \int_{h_c}^{h_{in}} \frac{dh}{V_d(h)} \quad (2.1)$$

The draining velocity  $V_d(h)$  is the reduction velocity of the film height dependent on the thickness.

### 2.1.2 Film Draining and Rupture

After droplet deformation and parallel film formation, the life time of the droplet is strongly dependent on the relative slow and gentle film draining. The surrounding liquid must be driven radial outwards of the gap before the two fluid bodies of drop and interface



can coalesce. If the gap width is reduced to submicron scale, molecules at the interface can rearrange allowing the coalescence to occur. In either case of colliding drops or the case of a single drop impacting a flat interface, the interaction time must be sufficient for the liquid film in the gap to drain. Otherwise, the volumes will not coalesce [Kassim and Longmire, 2004]. The classic Reynolds velocity for two parallel discs approaching each other in a viscous liquid, connects the thinning velocity  $V_{Re}$  to the driving force  $F$ , [O. Reynolds, 1886] and [Charles and Mason, 1960].

$$V_{Re} = \frac{2Fh^3}{3\pi\eta R_f^4} \quad (2.2)$$

For the stiff and flat disc shaped surface, film with radius  $R_f$ , and the dynamic film-viscosity  $\eta$ , it can be found for a droplet resting on a plane surface and deformed by it's own weight,  $R_f$  is obtained by considering the force on a droplet in equilibrium [Charles and Mason, 1960].

$$F = \Delta p \pi R_c^2 \quad (2.3)$$

$F$  is balanced by the pressure difference  $\Delta p$  from inside and outside the drop and the projected area with drop radius  $R_c$ . Substituting  $\Delta p$  according to Laplace's law gives:

$$F = \frac{2\pi\sigma}{R_c} R_f^2 \quad (2.4)$$

And for the case of droplet on a plane surface Eq.2.4 is reduced to

$$R_f = R_c^2 \left[ \frac{2\Delta\rho g}{3\sigma} \right]^{1/2} \quad (2.5)$$

where  $\sigma$  is the interface tension. Separation of oil and water is caused by a tension in the surface between the dissimilar liquids. This type of surface tension is called "interface tension", but its physics are the same.  $\Delta\rho$  is the difference in the density between the droplet and surrounding fluid and  $g$  is gravity acceleration. By substitution of Eq. 2.5 and Eq. 2.2 into Eq. 2.1 and integration, one obtains

$$\tau = \frac{\eta}{4} \left[ \frac{\Delta\rho g R_c^5}{\sigma^2} \right] \left[ \frac{1}{h_c^2} - \frac{1}{h_{in}^2} \right] \quad (2.6)$$

in most cases  $h_{in} \gg h_c$  so the equation reduces to

$$\tau = \frac{\eta}{4} \left[ \frac{\Delta\rho g R_c^5}{\sigma^2} \right] \frac{1}{h_c^2} \quad (2.7)$$

for the sake of argument, [Vrij, 1966] developed a formula giving  $h_c$  expressed by the Hamaker constant  $A_H$  which take the contribution of Wan der Waals forces into account

$$h_c = 0.268 \left[ \frac{36\pi^3 A_H^2 R_f^4}{6.5F\sigma} \right]^{\frac{1}{7}} \quad (2.8)$$

Dependent on film and droplet properties the coalescence time is now readily obtained in the flat disc approach. It has to be pointed out that some general limitations are present. First of all the deformation of a droplet in Eq. 2.5 has to be small, and the electrostatic repulsion  $\Pi_{el}$  between the film surfaces may be neglected. This is the case if double layers are not present, or if electrolyte content is high. In addition, the contribution of van der Waals forces  $\Pi_w$  are also neglected with respect to the capillary pressure  $P_0$  [Vrij, 1966].

Subsequent to film drainage and film rupture, collapse will eventually take place and is initiated by a hole formation in the separating film. The interfacial tension will as in the formation of the spherical droplet act to reduce the surface area.



Figure 2.4: *First, a small hole is formed in the film. The interfacial tension is immediately acting to minimize the film surface area and hence expands the hole which eventually will lead to collapse of the droplet*

As an estimation of the hole expansion velocity  $v$ , [A. Dupre, 1869] and referenced by [Charles and Mason, 1960] assumed that the energy released by rupture of a soap bubble is transformed into kinetic energy to the liquid suppressed by the expanding hole.

$$v = \frac{dr}{dt} = \sqrt{\frac{4\sigma}{\rho h}} \quad (2.9)$$

The properties are the soap film density  $\rho$ ,  $r$  the hole radius and  $h$  the film height. The formulas for coalescence time and film rupture are based on models and hence the equations should be used with care.

## 2.2 Droplet Breakup

Breakup of droplets is also a process that would be of interest for this study. As experiments in a "bottle test" is in the laminar regime, we will focus effects present in this kind of flow. The cause of breakup can be classified as one of five categories [M. Dhainaut, 2002]:

- maximum size with Kelvin-Helmholtz and Rayleigh-Taylor instabilities
- rapid acceleration
- turbulent fluctuations and collisions
- high shear stresses
- non uniformity in surfactant distribution

A non dimensional number often used in analyzing film flows and the formation of droplets is the Weber number. It is used when interface between two fluids are present and can be regarded as a measure of the importance of the fluid's inertia compared to its surface tension.

$$W_e = \frac{\rho U^2 d}{\sigma} \quad (2.10)$$

### 2.2.1 Kelvin-Helmholtz and Rayleigh-Taylor Instabilities

For the case of an interface between two fluids with different densities and with the heaviest on the bottom, Kelvin-Helmholtz instabilities can be generated. Two parallel fluids with different velocities might be sensitive to the slightest perturbation in velocity, it will generate waves and is the classic case examined.



Figure 2.5: A parallel stream with the heaviest fluid on the bottom  $\rho_2 > \rho_1$  and the with a relative velocity difference  $U_1 > U_2$

Rapid acceleration is one of the causes for droplet formation listed, it can be seen as a kind of Rayleigh-Taylor instability and will be treated along with it. The setup studied by Rayleigh consists of two parallel fluids with the heaviest on top and subjected to the gravity field as can be found in water balancing on oil. Small perturbations could trigger the system and release potential energy by growing into "fingers" as the fluids move into each other.



Figure 2.6: *Parallel stream with the heaviest fluid on top  $\rho_2 > \rho_1$ . As the instability develops, perturbations are rapidly amplified into penetrating Rayleigh Taylor fingers and a very distinct mushroom cape is formed*

While Rayleigh conducted the experiment in the earth's gravitational field, Taylor realized that the same situation is true when light fluid is accelerated into the heavier fluid independent of gravity.

## 2.2.2 Shear Stresses

Mixing of immiscible liquid/liquid systems is a well known industrial feature, it changes the properties of the product to the worse or better. As an basic step in mixing, deformation and breakup of droplets into daughter droplets at different immiscible liquids are important. Deformation is driven by imposed shear stress on the droplet in contest with the interfacial stress  $\sigma/R_c$ . The ratio between the deforming shear stress and the reducing interfacial area stress is expressed by the Capillary number

$$C_a = \frac{\mu U}{\sigma} \quad (2.11)$$

with the viscosity of the continuum phase  $\mu$ . For a small Capillary number the interfacial stress will dominate and a stable elliptic droplet shape exist. If the Capillary number is larger then a critical value, the droplet shape will be unstable and finally break. It is shown by [Grace, 1971] and [Taylor, 1934] that critical Capillary number is dependent on flow type and ratio between dispersed and continuous phase [Janssen, 1993].

### 2.2.3 Surfactants

Surfactants are compounds that reduce the surface tension of a liquid and the interfacial tension between two fluids, and can be coined as a blend of surface active agents. They are regularly used in dispersing, emulsifying and foaming agents and hence are of great interest for the oil industry. With decreasing surface tension, film rupture will be less likely due to reduced film drainage. The droplet is getting softer and increasingly adsorbs tangential stress from the film. The reduced surface tension forces will not be able to counteract large tangential stress and breakup will take place. Surfactants act as di-polar elements and are structured with either the hydrophilic head or hydrophobic tail towards its surrounding fluid. Surfactants adsorb at the interface and hence reduce the local interfacial tension, by film draining, surfactants can be washed away and hence the local interfacial tension is now increased. From this a back flow of surfactant-containing film liquid can arise, once again reducing the interfacial tension but now also increasing the film. This effect is known as the Marangoni convection [M. Dhainaut, 2002].

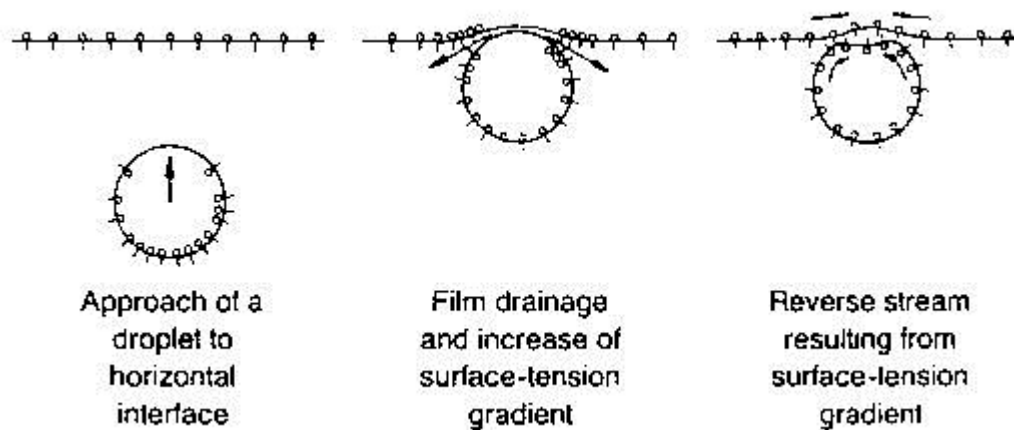


Figure 2.7: A bubble is traveling through a aqueous solution in a system with surfactants. Hindered film drainage and film backflow due to change in interfacial tension is indicated

## 2.3 Terminal Velocity

A dispersed droplet of water propagating through a oil phase is illustrated in figure 2.2. The counter-current drag force and gravity force are working on the droplet until it stabilize at the terminal velocity. The drag force acting on the droplet is a function of the Reynolds Number.

$$Re = \frac{\rho_s V_t d}{\mu} \quad (2.12)$$

The terminal velocity is defined  $V_t$ ,  $\rho_s$  is the droplet density,  $d$  the diameter and  $\mu$  the fluid dynamic viscosity. The terminal velocity for dispersed particles can be expressed by the following equations at different regimes [Perry, 1950].

For low Reynolds number between 0 and 2, the velocity is given by Stoke's Law.

$$V_t = \frac{g D_p^2 (\rho_s - \rho)}{18\mu} \quad (2.13)$$

Where  $g$  is the gravity force and  $\rho$  is the fluid density. Stoke's law is applied for small droplets and high viscosity liquid phase. For Reynolds number between 2 and 500 the Intermediate Law is valid and often used for medium sized droplets.

$$V_t = \frac{0,153 g^{0,71} D_p^{1,14} (\rho_s - \rho)^{0,7}}{\rho^{0,29} \mu^{0,43}} \quad (2.14)$$

Last, the Newton's Law is valid for Reynolds number between 500 to 200.000. It is mainly applied to large droplets and particles.

$$V_t = 1,74 \sqrt{\frac{g D_p (\rho_s - \rho)}{\rho}} \quad (2.15)$$

In the preliminary studies the size dependent terminal velocity was investigated experimentally and compared to the models above. The droplets were produced in four different sizes, ranging from about 1.5 mm to 3.5mm in diameter. Droplet diameter versus droplet velocity is plotted and compared to the three models: Stoke's law, the intermediate law and Newton's law.

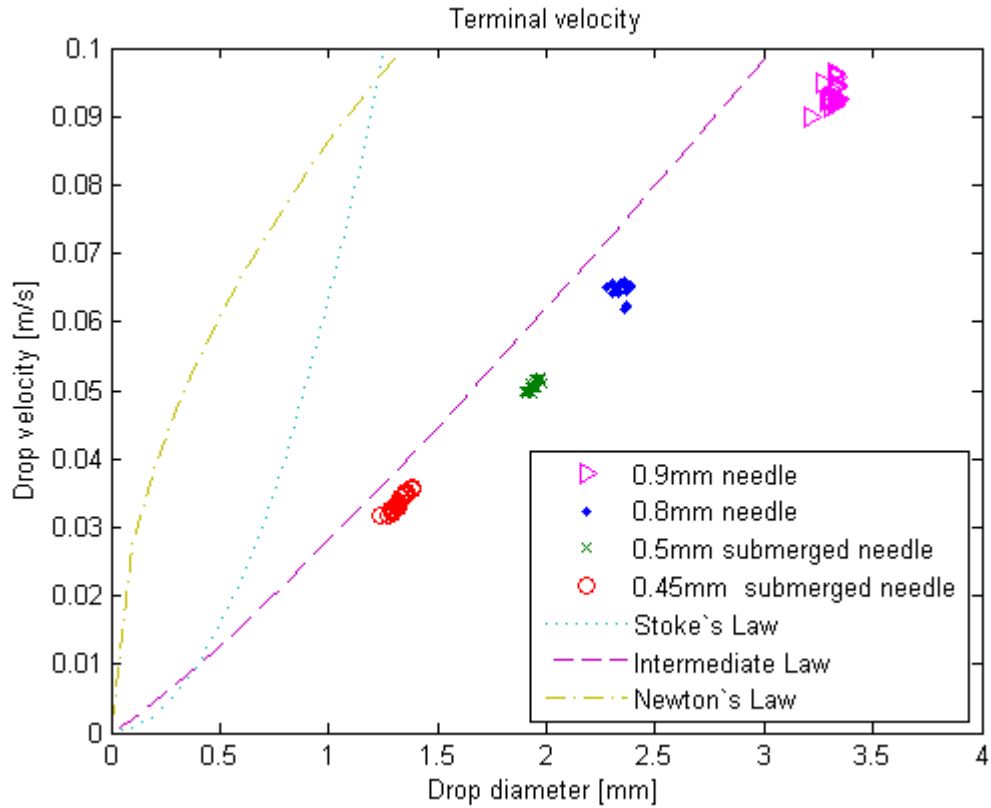


Figure 2.8: Terminal velocity for droplets produced by 4. needles of different sizes

The size dependent terminal velocity corresponded well to the Intermediate law, predicted by the Reynolds number. Some minor deviation from model and experimental results are present, but the trend-lines are the same. On the basis of the previous results it is assumed that Stoke's law can successfully predict the microdroplet terminal velocity giving speeds up to 0.01 m/s.

## 2.4 Micro Size Droplets Generation

Many processes and devices are making use of small droplets to perform their task, a very common application is in the ink printer where tiny droplets are generated and transferred to a sheet of paper. The ink printer is relying on the use of pressure pulses in order to generate drops [Wright et al. 1993], by pressure ejection the drop diameter is closely related to the orifice size. Generation of very small droplets could be useful in masking, producing small beads, chemical and biological sampling, but would require small capillaries and orifices which are difficult to manufacture, fragile and exposed to clogging. Electric spraying on the other hand is using the ability of electric forces to deform a meniscus and produce droplets considerably smaller than the orifice. Electrostatic forces can act upon

the liquid surface rather on the the fluid as a whole and are thus vastly different from the pressure pulses that are acting upon the whole fluid body. Electrohydrodynamic spraying can be divided in two main categories, cone-jet and drop periodic mode. The cone-jet mode produces a fine spray of drops but are not particularly suited for droplet generation and drop periodic mode is whenever drops are produced one by one as in dripping. It is worth noticing that both modes produce electrically charged droplets that would affect the coalescence process of e.g. a water/oil system. In the current paper by [Wright et al]. they proposed to use voltage pulse in cooperation with pressure pulse to generate single droplets, they showed that single pressure pulse can trigger a drop ejection.

In the work of [Atten et al. 2008] a single non-charged water droplet in oil is obtained by applying a voltage pulse on a conductive liquid meniscus, it deforms, makes a neck and breaks up. The behavior and generation of such a droplet are investigated further by [Raisin, 2011] which successfully produced and captured microdroplet generation. An image sequence taken from this work shows the deformation and ejection of a droplet from a meniscus, the diameter of the ejected drop is about  $238 \mu m$ .

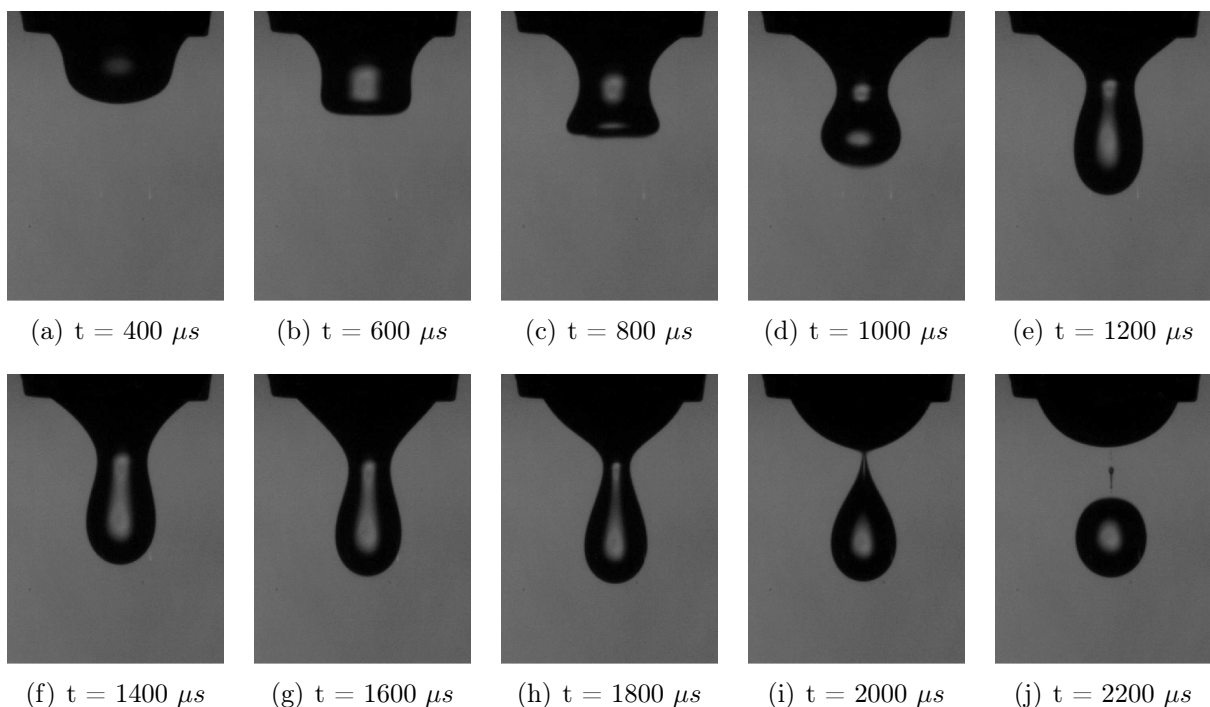


Figure 2.9: *Deformation of meniscus and ejection of a droplet, [Raisin, 2011]*

The transient electrically driven deformation of the water/oil interface is shown, the meniscus starts of with a regular smooth shape, but is clearly affected by electrical forces flattening the meniscus surface. The third frame in particular shows a special behavior with a neck and flat tip not observed previously. After the neck is formed, deformation continues



and the meniscus splitting takes place a few hundred microseconds after the end of the pulse (between frames 7 and 8), leaving enough time for the charges to relax and ensuring the electroneutrality of the drop. After deformation and necking, gravity is left to do the work of separating droplet from meniscus. Small satellites, resulting from the break-up of the water ligament, are observed in the final frame and needs special attention. Satellites are most frequent after injections of relatively large drops. The only pressure acting upon the meniscus in this case is the electrostatic one,

$$P_{es} = \frac{1}{2}\varepsilon E_n^2 \quad (2.16)$$

$E_n$  is the normal component of the electric field and  $\varepsilon$  is the oil permittivity. A distinct electric pulse is produced as square as possible to reduce the lead and trail time, however in a later publication from [Raisin, 2011] it was shown that a square pulse were not optimal to produce a consistent and wide range of droplet sizes and an alternative pulse profile was developed (MSP), but for now we will stay with the square pulse. A sketch indicating the main geometrical parameters is made in figure 2.10 and is showing a capillary tube, meniscus and electrode.

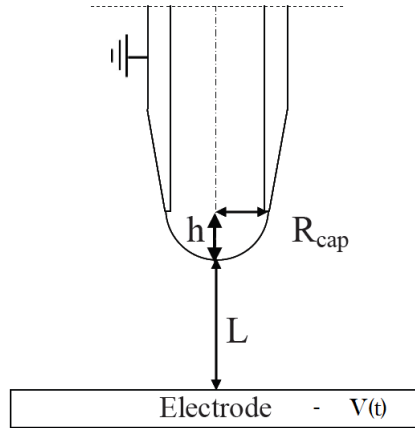


Figure 2.10: *Main geometrical parameters*

The meniscus height is given by  $h$ , the capillary radius by  $R_{cap}$  and the distance between the meniscus and electrode is given by  $L$ . With respect to the forced pulse amplitude  $V$ , a minimum for deformation can be defined by balancing the electrostatic and capillary pressure  $P_{cap}$  on the meniscus surface

$$P_{es} = P_{cap} \quad (2.17a)$$

$$\frac{1}{2}\varepsilon E_n^2 = \frac{2T}{R_{cap}} \quad (2.17b)$$

where  $T$  is the interfacial tension coefficient. Instability and break-up appears in the region of the highest field. An estimation of the maximum field intensity of a hyperbolic with  $R_{cap}$  as radius of curvature, is given by:

$$E_{max} = \frac{2V}{R_{cap} \ln\left(\frac{4L}{R_{cap}}\right)} \quad (2.18)$$

The voltage can be estimated by replacing  $E_n$  in equation 2.16 with  $E_{max}$ .

$$V_{low} = \sqrt{\frac{TR_{cap}}{\varepsilon} \ln\left(\frac{4L}{R_{cap}}\right)} \quad (2.19)$$

The electric field pulse based injection of a charge free drop requires the supply of a large amount of energy in a very limited time to the water meniscus. Applied potential differences  $V$  higher than  $V_{low}$  might thus be necessary depending on the pulse duration.

Next, the pulse duration is estimated, the electric pulse should have finished before the droplet break free in order to produce a neutral droplet. This would be at the point of a liquid filament appearing between the drop and meniscus. To prevent producing a charged drop the pulse duration  $\Delta t$  should be less then the characteristic capillary time  $t_{cap}$ :

$$t_{cap} = \sqrt{\frac{\rho R_{cap}^3}{T}} \quad (2.20)$$

A modified Weber number was introduced by [Atten et al. 2008] to compare water drop injections using square voltage pulses of different duration and amplitude. The expression represents the work of electrostatic forces acting on a non-deformable meniscus.

$$W_e^* = \int V(t)^2 dt \quad (2.21)$$

### 2.4.1 Multi-Stage Pulse

The Multi-Stage Pulse (MSP) is described by the rising edge and plateau of a trapezoidal pulse providing a fast and controlled deformation of the meniscus mandatory to avoid the aforementioned cone formation. Then, the voltage intensity decrease during the trailing edge prevents the multi-jet spraying and lets interfacial tension bring back the maximum elongation at the axis. Finally, a DC offset is applied resulting in a new trapezoidal pulse so that electric forces overcome interfacial tension forces and detach a drop. This pulse design provides several possibilities to tune the signal, by adjusting the duration and amplitude different droplet sizes can be obtained.

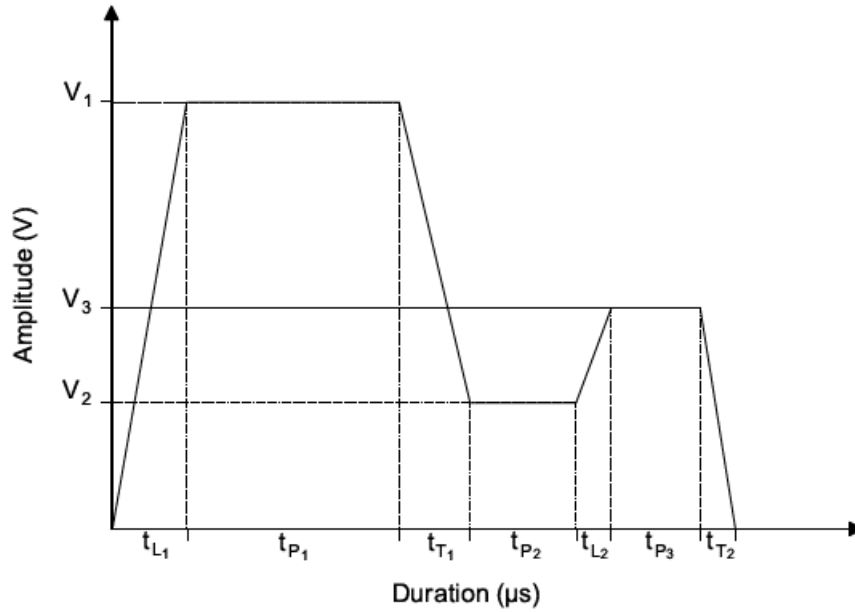


Figure 2.11: *Typical profile for a Multi-Stage Pulse*

Three amplitudes  $V_1$ ,  $V_2$  and  $V_3$  are present with their respective  $t_L$ -lead,  $t_P$ -pulse and  $t_T$ -trail time. In total 9 different parameters are adjustable and hence gives a vast range of tuning opportunities. The profile for the Multi-Stage Pulse in figure 2.11 is typical for a configuration obtaining a good reproducibility and wide variation of drop diameters ranging from 30-200 micrometers [Raisin, 2011]. In the end, parameters needs to be adjusted for each unique experimental setup but equations 2.20 and 2.19 gives useful estimations.



## Chapter 3

# Requirements and Specification for the Design of the Experimental Facility

The ultimate goal of this project has been to build a facility that can generate and record droplets that are coalescing on a planar water/oil interface. The facility needs to accurately allow change of droplet size and produce stable homogeneous droplets at every size. In addition, the event of coalescence has to be captured at the interface with an image quality that can be processed by a software.

The main requirements and specification for the design of the facility are the following:

- Fluids, two set of fluids are considered, water and Exxsol D80, and water and petroleum. The water/Exxsol D80 system is transparent and easy to operate in the visible region, while the water petroleum system needs to be study in the near infrared region.
- The droplet size aimed for is in the range of 50 microns to 1000 microns. This broad size range is covered by using a syringe pump with needles of different diameter for the larger droplets, while for the smaller ones a high voltage droplet generator is needed which is designed in this thesis.
- Illumination and visualization: the facility has to provide access to different lighting and visualization systems.
- Control and automation of the experiment: the experimental setup must repeat the experiment hundreds of times for a given fluid sample. This imply to automatically control the experiment i.e. the generation of the droplet, detection of the moving droplet and capturing.
- Data processing: the sequence of the images needs to be processed and the coalescence time determined automatically.



# Chapter 4

## Results and Discussion

This section present an overview of the tests and calibrations performed on the designed test facility.

One of the main component designed during this thesis was the droplet generator, unfortunately due to an factory issue the high voltage power amplifier has been returned to the factory for repair and service without being able to test the performance.

As a summary, the main sub-systems designed were:

- Micro size droplets generated by a high voltage unit.
- Droplet detection.
- Visualization unit.

In addition, the study included benchmarking study of:

- Illumination.
- High speed visualization.
- Data acquisition chain.

### 4.1 Micro Droplet Generation

Micros size droplets were intended produced by a high voltage amplifier in co-operation with two electrodes in the visualization unit. The whole facility was assembled and the high voltage amplifier was connected to the needle and to the base electrode by cables. The unit was turned on at a low voltage - to low for anything to happen, merely for testing purpose. Everything worked fine and the high voltage amplifier was turned of for adjusting the facility. After completing adjustments, the power level directed to the amplifier was

increased and the unit was ready to be turned on again. Before conducting voltage, the amplifier is started by putting on the power and then by pressing a voltage ON switch, it was not possible to start the amplifier and product support was contacted. On their request a long list of about 20 possible bugs were checked to discover any errors, finally it was concluded that no physical damage like burned fuses or wires was visible, nor was any noise or smell present, indicating malfunction of the unit. The amplifier is returned to producer for service.

## 4.2 Droplet Detection

Detection of falling droplets is important for the recording process. By capturing one droplet at the time instead of continuously running the camera, droplet properties can be connected to a distinct sequence, allowing to easily go back and study interesting cases, discover possible trends in coalescence and save a lot of space for data storage. Limited internal memory is also a issue when using high speed cameras and could result in failure of recording the actual coalescence as the memory runs out. We aim to build a facility that can generate very small droplets, and to register passing droplets it requires a very high accuracy of laser and detector. A rigid structure was designed and build to ensure that laser source and detector are completely in line and that future modifications can be done to the setup without worrying about ruining the alignment of the two. The module is completely removable and allows flexibility in finding the optimal arrangement relative to the rest of the setup. The module is shown in fig 4.1 including shutter, lenses and fiber-optics.

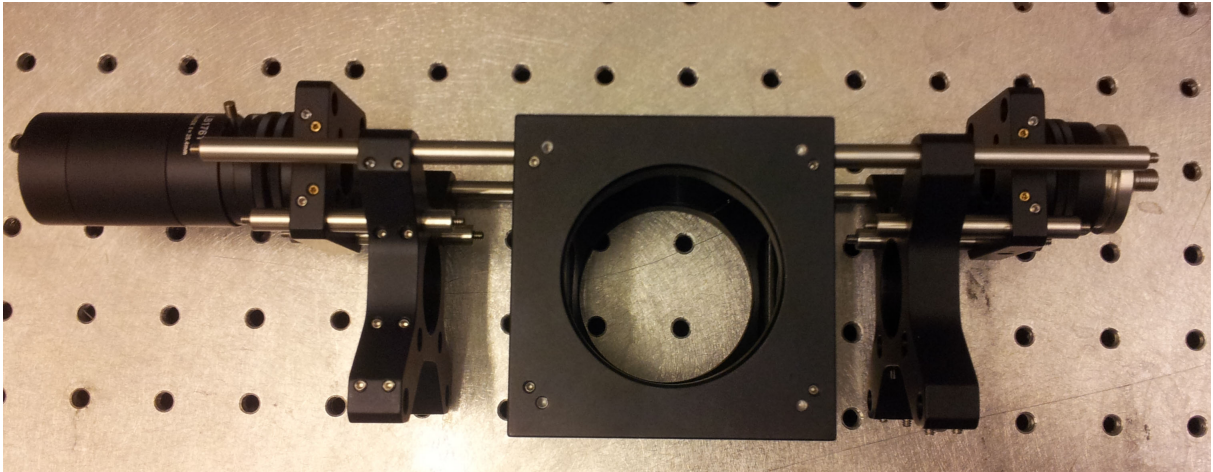


Figure 4.1: *Droplet detection module, the laser beam is entering on the left side, passing the cage, collected and exits on the right side*

The whole module is constructed around a 60 mm cage system cube with  $\text{Ø}50$  mm holes in which the container is inserted. On two opposing sides of the cube are in total four  $\text{Ø}6$



mm cage assembly rods attached, two on each side. 30 mm to 60 mm cage plate adapters are applied on each side along with two new sets of Ø6 mm cage assembly rods. The rods are now matching 30 mm cage systems and a threaded 30 mm to 16 mm cage adapter plate is mounted allowing for an adapter with external SM05 (Ø1/2") threads and internal SM1 (Ø1") threads to be attached. Optics in use are all having Ø1", by combining common male and female couplers they can readily be attached to the module.

The beam transmitter side is built up by a SMA fiber adapter plate with Ø1" external thread, Ø1" lens tube, a Thorlabs LB1761 BI-Convex lens with focal distance  $f=25,4$  mm for collecting the beam, a lever-actuated iris diaphragm for governing the beam size and finally a lens tube coupler with external threads. The build up of the receiving side is done in the same way but somewhat simpler. A lens is integrated in the fiber adapter plate with Ø1" external threads in order to collect the laser beam and by applying a Ø1" lens tube and a lens tube coupler it can be attached to the module. The laser light is provided by an adjustable Thorlabs S1FC635 Fiber Coupled Laser Source with key-switch and transported by a fiber-optic cable attached to the transmitting side of the module. A power level of about 2 W is sufficient to detect passing droplets. On the receiving side another fiber-optic cable is transporting the laser light to a Thorlabs DET10A/M SI detector.

An appealing feature and side effect of using the laser beam as a detector is that it assures the falling droplet being at the same depth relative to the camera every time. Small movements relative to the camera focal point would greatly deteriorate the image quality. Greater droplets or droplets released on top of the oil surface show a tendency to travel in the horizontal plane, ultimately resulting in coalescence somewhere away from the focal point. The laser beam is in this way effectively controlling to position and path of the droplet. The need for detecting a droplet is fulfilled by this module, but it also sets some of the premises for the visualization unit, as it has to be inserted into the 60 mm cage. The walls can at maximum be 35 mm wide to fit inside the circular hole with a diameter of 50 mm.

The droplet detection unit is working as it should and easily registers droplets with a diameter of *mm*. It is a very stable and rigid structure that ensures the laser emitter and detector to be aligned. By adjusting the power and iris the laser beam is adapted to droplet size. With the help of an amplifier it successfully produces signals of 1 - 5 V which are the requirement of making the BNC / Signal Generator to operate. The trigger signal produced from the detection unit and the signals generated from the BNC to camera and light source is visualized by the oscilloscope.

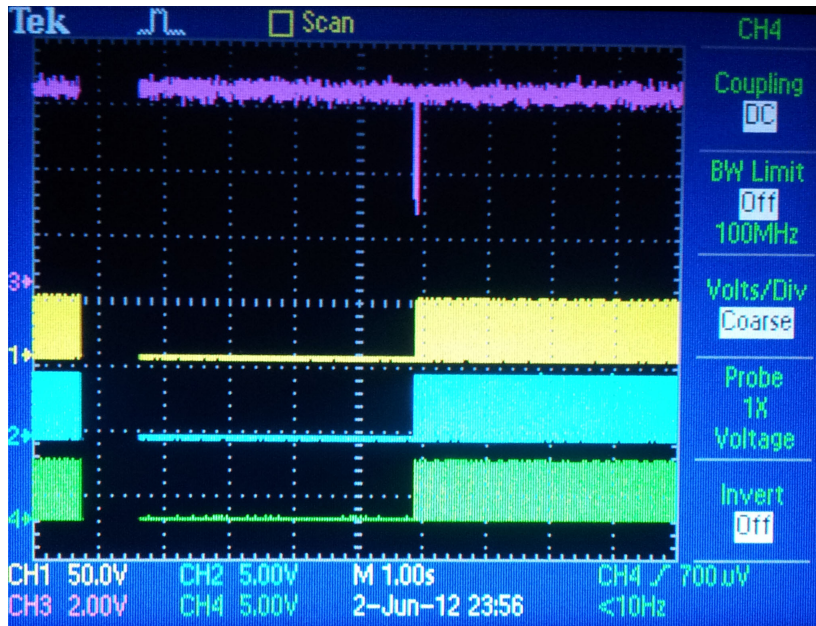


Figure 4.2: *Input signal by a droplet triggering signal production of 400 pulses per second to camera and light source visualized by an oscilloscope*

The top line with one distinctive drop is from the detection unit, when the laser beam is interfered, a signal of about 4 V is produced. At the moment the signal from the detection unit is received, the BNC start to produce it’s own signals. What appears as 3 thin lines shifted to thick lines are the signals sent to the camera and light source, made at a rate of 400 pulses per second. Witch in turn produce an evident proof of the successful triggering, by video recording and light emission.

### 4.3 Illumination

Correct and fine tuned lighting is a very important part of visualizing droplet experiments. It is decided to use pulse-illumination instead of continuously-illumination due to the ability of short pulses to “freeze” the motion of fast-moving objects in the camera image, giving qualitatively better images. The control units for all illumination sources revised are accepting external input of pulse shape and except power level and accuracy they behave identical. It is important to realize that when using pulsed light with high speed cameras, the duration of the flash from the source determines the exposure time – the camera exposure time is not relevant. A well matching source gives better quality images in form of brighter frames and clearer borders between drop and surrounding liquid. A wide range of Thorlabs Mounted High Power LED diodes at different wave lengths and Thorlabs High Power LED Drivers with maximum output current of 1200 mA and 2 A are available for studying the coalescence mechanisms. In a water/Exxsol D80 system most combinations of diodes and control units perform decent. The boarder between water and

Exxsol D80 is nicely visualized and the control unit accepts trigger signals and any given light-profiles (fps) forced by the BNC trough the MOD IN port without any hassle. Combinations of control units and diodes with visible white light, near infrared - 850 nm and red wavelengths of 625 nm are tested and found sufficient to perform basic investigation of the coalescence mechanisms in the water/ Exxsol D80 system. No significant differences between the combinations of diodes and controls were found.

Search and application of an alternative light source was motivated by the desire to obtain higher quality images and possibly even study the interaction of water and petroleum directly. For this purpose it was decided to use an Oxford Firefly 300 W laser, emitting infrared light at wavelengths of 805nm-810nm. The unit is mounted on to the assigned board and the flexible light guide and camera is aligned. Equipment initiation testing was performed under supervision, it turned out that the corresponding interlock had to be recovered before the unit was ready for experiments. Due to the application of a high-power laser, training and special safety measures needs to be taken. Moderate and high-power lasers are potentially hazardous capable of burning the retina of the eye, or even the skin by relatively small amounts of laser light. Skin burn, or permanent eye damage can be a result of direct, diffuse or indirect beam viewing. High-power lasers may ignite combustible materials, and thus may represent a fire risk. These hazards may also apply to indirect or non-specular reflections of the beam, even from apparently matte surfaces - meaning that great care must be taken to control the beam path. The laser with all it's component is shown in figure 4.3.

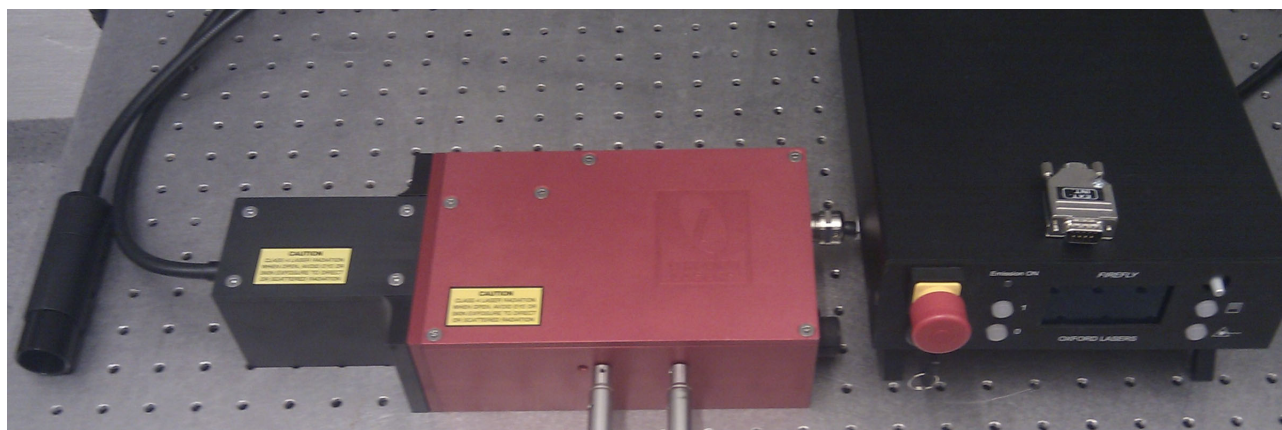


Figure 4.3: *The flexible light guide to the left, in the middle is the beam generator and to the right is the control unit with the safety interlock lying on top*

The control unit of the high power laser is equipped with a key switch, radiation button, emergency button and a safety interlock. As a last action the generator is equipped with a physical barrier that needs to be opened to let the beam pass, additional measures are mandatory safety goggles, red signal lamp and sealed area when the laser is in use. An enclosure is build around the laser to minimize reflections and is effectively reducing the

risk of exposure. The infrared laser beam is invisible which complicates the operational procedures as the beam and any reflections needs to be detected by a infrared sensitive safety card.

Testing of a petroleum/water system was done by filling a cuvette with petroleum and insert a drop of water to it. Unfortunately it was not possible to detect any light emitting from the cuvette. Power was set to maximum but the images recorded from the event all appeared dark. The hope was that intensity of the laser could compensate for the suboptimal wavelengths of 805nm-810nm. While the high power laser failed to successfully complete petroleum/water experiments the results for the water/Exxsol D80 case was better with higher quality images and greater contrasts in particular.

### 4.3.1 Absorption Spectroscopy

An appealing idea is to directly study the interaction between water and petroleum, and as a response to the failed cuvette - high power laser experiment, it was decided to investigate what could be done to improve the result. As the laser is emitting infrared light at a wavelength of 805-810 nm it was assumed that it successfully could shine trough the very dark and dense petroleum. Based on the previous tests it seemed difficult, but absorption spectroscopy was performed. A Thorlabs CC5200 spectrometer is used in combination with a Thorlabs Mounted High Power LED diode to see which intervals of wavelengths that are absorbed by the petroleum. Small quartz cuvettes of thickness 2 and 4 mm are filled with oil and the emitted wavelengths are measured:

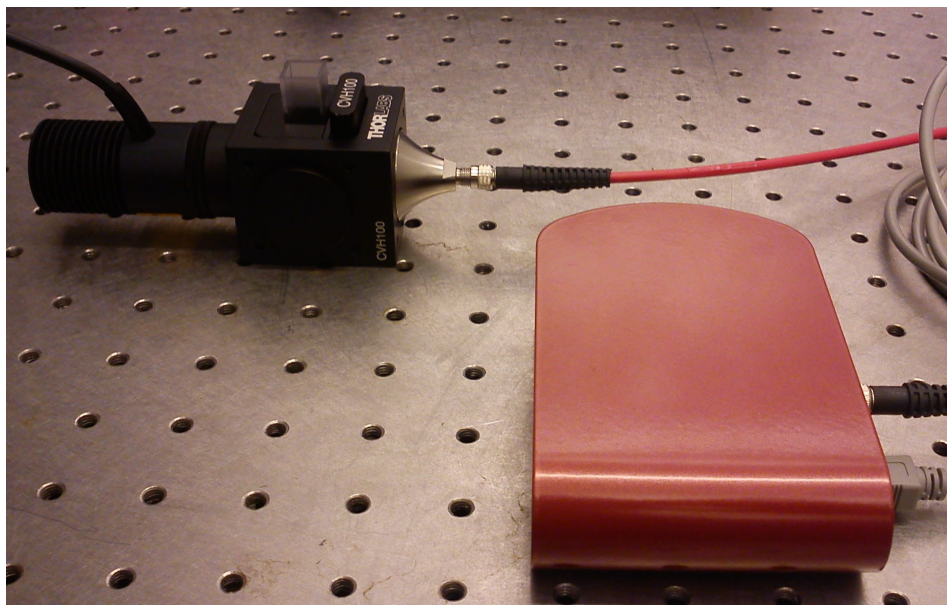


Figure 4.4: *Cuvette holder, light source, cuvette filled with oil and computer connected spectrometer*

The light detected by the CVH100-COL - fiber adapter with lens mount is sent to the software for processing. In the user interface, different options are available to better explore the results. A very useful feature is to compare different signals relative to each other, different liquids and time integrals can easily be compared. Intensity on the y-axis is plotted against the wavelength nm on the x-axis. Two samples, one of heavy and one of light petroleum are provided and are measured by the spectrometer.

Absorption spectroscopy is used to determine which wavelengths of light that are best suited in the experiment. A Thorlabs Mounted High Power LED white light diode are tested with a 2 and 4 mm thick cuvettes filled with the two samples. White light contains a broad specter of wavelengths making it possible to identify the most suitable range. The experiments are made and the result is that no light is transmitted. Not even at integration time of 5000 ms is it registered any light passing the thin layer of petroleum. As expected the LED is not powerful enough and the pitch black oil is absorbing all the wavelengths.

The light source is changed to the laser to see what effect it has on the emitted spectra. The top line is the reference case with no cuvette present and integration time at 1 ms. The bottom line is with a 4 mm thick cuvette filled with light-oil and integration time of 5000 ms

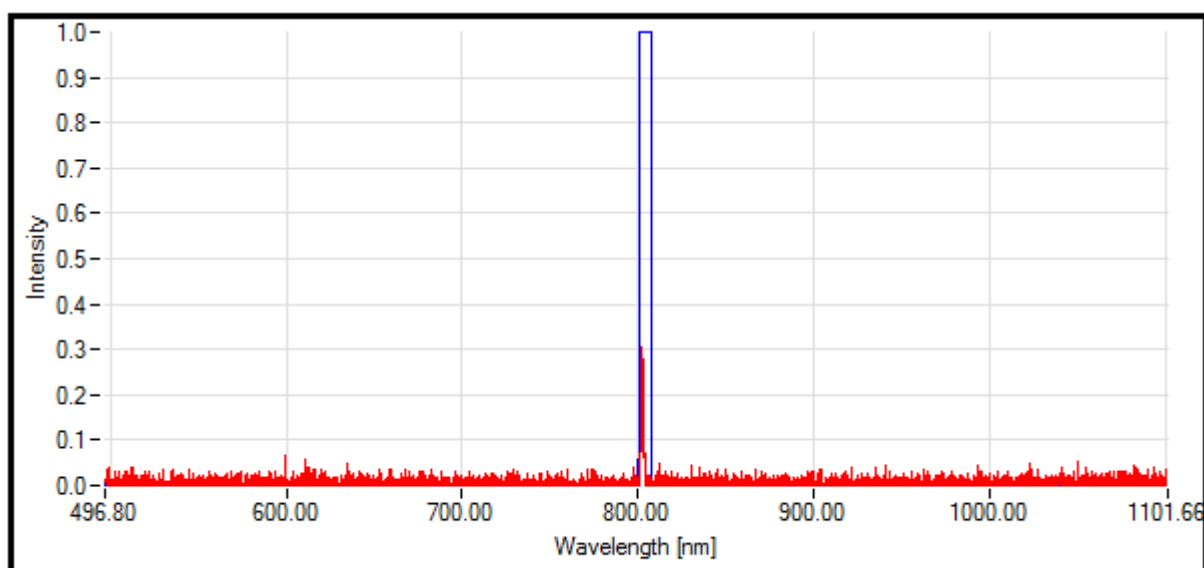


Figure 4.5: *Infrared laser, light petroleum and cuvette thickness of 4 mm*

A very narrow spectrum is observed for both the reference and time integrated lines. The spectrum for the case of no cuvette in the top line is evolving around 805 nm with sharp edges and fully saturated at intensity 1. With cuvette present the bottom line peaks at an intensity about 0.3, this behavior is as expected due to the laser specifications of wavelengths in the region of 805-810 nm.

As the characteristics of the light oil has been tested, the same research is conducted on the heavy oil. Laser light in combination with heavy oil give a profile with the reference on top and the case of a cuvette filled with oil at the bottom. The cuvette is 2 mm thick, filled with heavy petroleum and integration time is 5000 ms, the reference case apply 1 ms integration time.

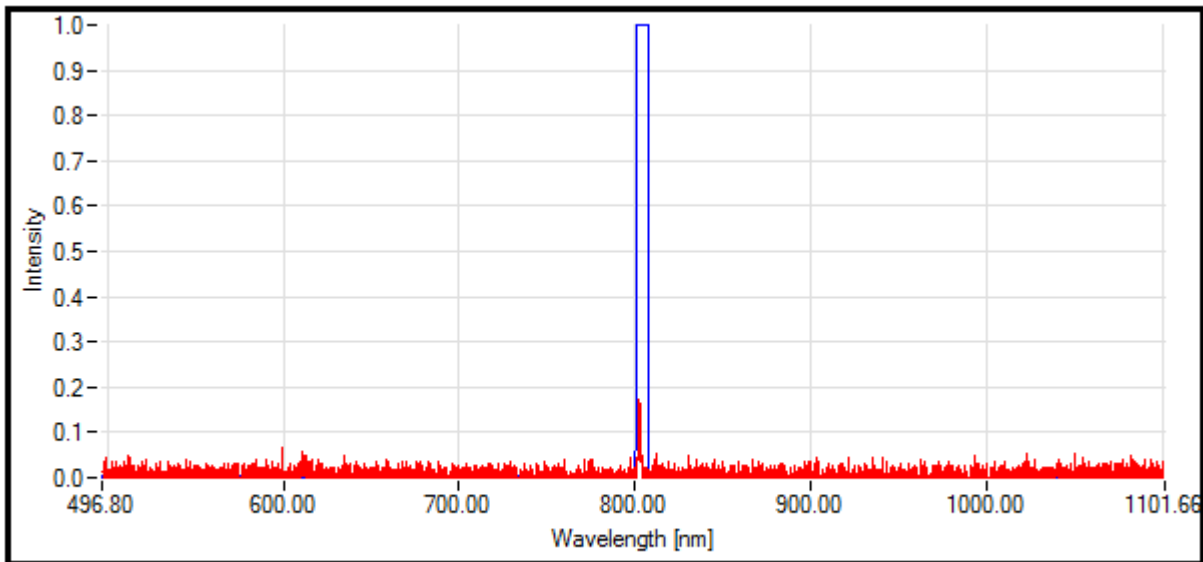


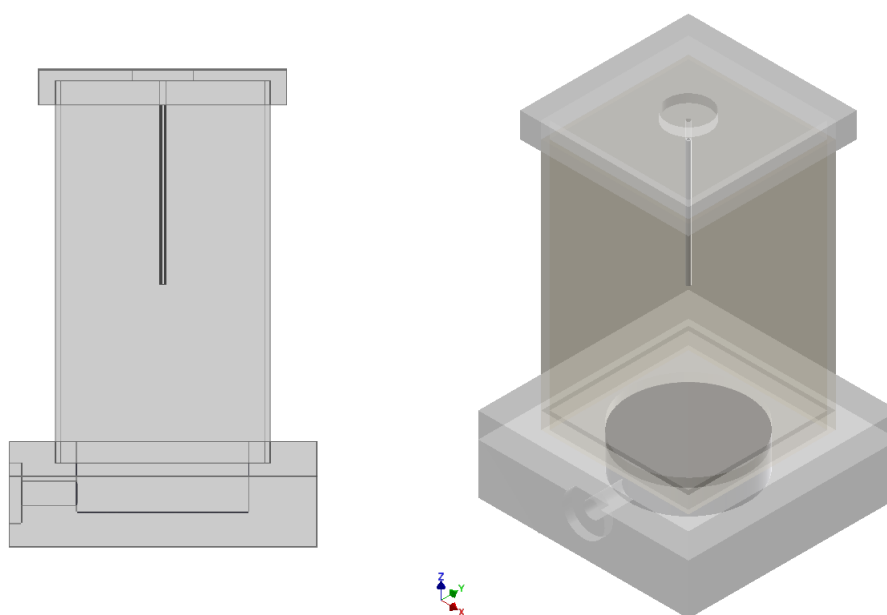
Figure 4.6: *Infrared laser, heavy petroleum and cuvette thickness of 2 mm*

Again a very narrow spectrum is observed for both the reference and time integrated lines. The spectrum of the reference is evolving around 805 nm with sharp edges and fully saturated at intensity 1. The bottom line peaks at wavelength 805 nm and intensity about 0.15, the behavior is very similar to the light-oil case but less energy is transmitted and the intensity is about half of the light-oil even with a cuvette thickness of half the size. It seems clear that even though both samples appear the same, the heavy oil absorbs much more energy than the light oil. It is also evident that the powerful laser is not even able to shine through oil thickness of 2 mm, making testing of water/petroleum hard.

## 4.4 Visualization

One of the main project targets is to construct the visualization unit for micro size droplet generation. The construction of such a unit in its simplest form demands a certain complexity as it needs to meet several challenges. Firstly, and most importantly is the micro size droplet generation, by the help of a high voltage amplifier. In order to produce the voltage pulses for creating the droplets, a second electrode in addition to the conductive

needle is integrated. The electrode should be in direct contact with the fluids inside the column and needs a safe connection point to avoid any hazardous situations. Secondly, it is really important that the processes inside the visualization unit can be captured properly, as the images are the basis for any analysis of coalescence. And third, the dimensions have to match the droplet detection module. A model of the visualization unit is made in Autodesk Inventor and explained further:



(a) A 2D-model of the visualization unit

(b) The visualization unit in 3D

Figure 4.7: The full model of the visualization unit with all the basic parts present

the unit is made up by several basic parts with a lid, needle, fluid container, base and an electrode. The lid has no other function than to seal the container and support the needle. It is made of PVC with cuts that matches the dimensions of the fluid container, a small hole is made through and through in which the needle is inserted and an extrusion is made on the surface to allow additional support to be attached. Next is the fluid container, it is shaped as a rectangular prism and made out of glass. A cylindrical shaped tube would be much easier to get a hand on, but straight walls were chosen to remove as much uncertainties as possible to how light was bent, passing the glass walls. Due to the shape and size, the unit is handmade by a glass-workshop and produced in three different lengths so the optimal one could be found by testing. The rectangular prism is made with an "open" design, only the sidewalls are present leaving the top and bottom open. The top is open to allow liquids to be poured in and removed on a later stage, the bottom could easily have been sealed with a glass plate that would remove the need for making a base, but is

left open for two main reasons. Number one, future modifications like allowing circulation of liquids and adjustments to the electrode are much easier done to the base made of PVC than the glass walls and number two, cleaning of the prism is made much easier. Imaging petroleum being inserted to the prism, it would be a tedious work removing it from all the corners and bends and it is therefore left open.

The electrode is a circular unit made of steel and integrated with the PVC base. It is important that the base can provide a safe and well functioning connection point from the high voltage power amplifier to the electrode. Similar to the top, cuts are made in the base that match the prism so it can easily be inserted. The tracks are lined with rubber to seal the tracks and assure that water and oil are not leaking while the experiments are running. In figure 4.8 the first version of the visualization unit ready for experimental work is shown.



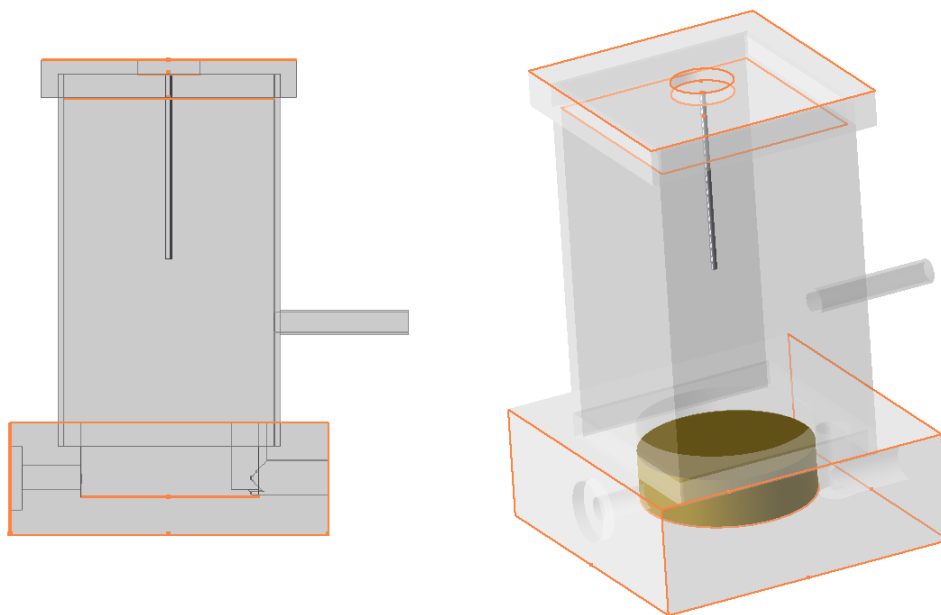
Figure 4.8: *Final visualization unit used in the experimental setup*

Starting from top, a blunt needle with a yellow cap is attached to a tube providing water and is inserted through the center of the lid into the oil phase of the visualization unit. The needle is grounded by a wire extending to the high voltage amplifier. The walls of the visualization unit are made of glass and glued together, inside the unit there are three phases, on top is air, next is Exxsol D80 and from the middle and down is water. A



distinct interface of air and oil can be observed, and just at the tip of the needle a water droplet of about 3 mm in diameter is formed. When the droplet is released it will fall to the water/oil interface and coalesce. An electrode in direct contact with water is placed in base of the unit, a connection point is made by making a threaded hole through the PVC base and into the electrode. A screw is inserted and a cable from the high voltage source is attached and insulated. Finally, the unit is mounted rigid to the table by two clips. The original plan was to make the base removable, but after a lot of trail and error in the workshop, witnessed by the hole in each corner of the base without any function, the plan was rejected. It was decided to glue the base and glass together and develop the design on a later stage.

Although not explored in more detail, some future modifications to the visualization unit seems reasonable. As temperature gradients play an important role in droplet coalescence, fluid temperature control could be important to obtain results under standard conditions. However, allowing fluid circulation must be done under great care as even low flow rates could result in change of conditions outweighing the benefit of homogeneous temperature. A first proposal for an updated design is made in figure 4.4.



(a) 2D model of updated visualization unit (b) 3D model of updated visualization unit allowing for temperature control

Figure 4.9:  
*Modified visualization unit with an added glass tube to the wall and extracting channel to the base*

The most noticeable change is made to the glass container where a point of fluid insertion is added. The receiving pipe is made out of glass and allows tubing to be attached.

Thermostat controlled fluid is inserted at this point while fluid is extracted from the base. By looking to the 2D and 3D model a new extrusion is made to the base allowing fluid to exit. By using this arrangement with insertion on top and extrusion on the bottom, the water phase stays stratified and minimal fluid bulk motion is induced. Finally, the PVC base itself is made out of a single piece instead of two separate pieces for simplicity. The intended reason for making it of two pieces was for cleaning purpose but did not outweigh the extra work of making the base.

## 4.5 High Speed Visualization

Selection of camera to record the droplet experiments is a never ending battle between accuracy and complexity. In total four different cameras have been up for evaluation through preliminary studies and experimental phase. Two cameras, a Thorlabs Smart High Sensitivity CCD Line Camera and a Appsintech CamIR 1550 infrared camera were rejected at a early stage due to insufficient resolution ( only one pixel in height ) and operational difficulties, respectively. Remaining are the Thorlabs DCC1645C High Resolution USB 2.0 CMOS Camera and Photron Fastcam SA3 high-speed camera with very distinct pros and cons.

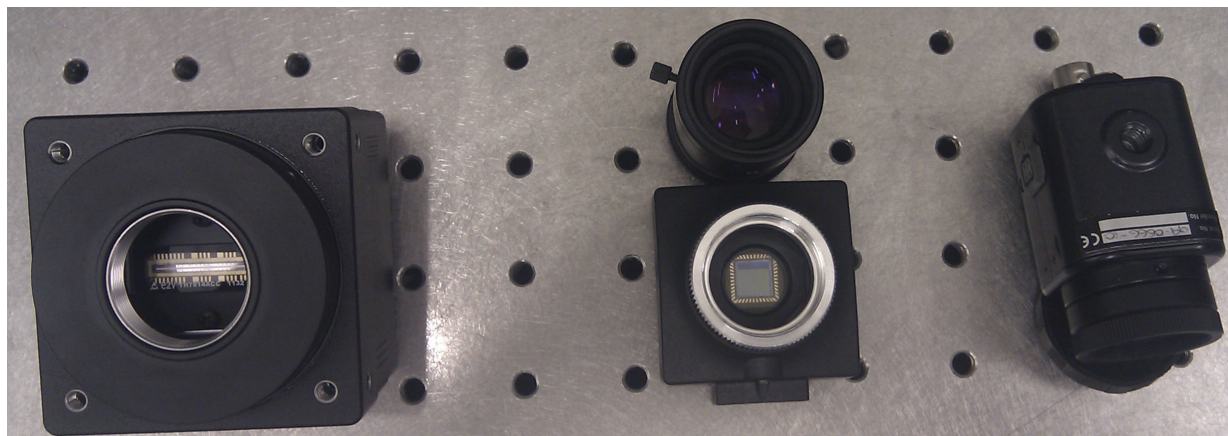


Figure 4.10: *From left to right, Thorlabs Smart High Sensitivity CCD Line Camera, Thorlabs DCC1645C High Resolution USB 2.0 CMOS Camera with external lens and Appsintech CamIR 1550 infrared camera*

The Photron Fastcam SA3 camera is as the name indicates a high speed camera with a possible frame rate of  $\mathcal{O}(10^4)$ , flexible shutter and greatly adjustable focal point. However, a major drawback is the 2 gigabyte limited internal memory of the camera, at suboptimal resolution and frame rate it is a real risk of running out of memory and not capture the entire coalescence process. The sheer size of the total amount of data acquired by an experimental series is less of a problem, although it needs some attention. A new

stationary computer is acquired to handle the data from this and related projects, and effectively solves the storage issues. In addition, drivers needed to automatize the setup in LabVIEW are shown to be very unstable which could be problematic. The last camera, Thorlabs DCC1645C High Resolution USB 2.0 CMOS Camera is much less sophisticated with a obtainable frame rate of  $\mathcal{O}(10)$  and limited possibilities of adjusting the focal point depending on the external lens. Regardless of the less attractive properties relative to the high speed camera, it does not have the risk of running out of internal memory as all data is stored directly on the computer. This is vital as missing some samples would ruin the experiment and trustworthiness of the final conclusion. Also, the Thorlabs DCC1645C High Resolution USB 2.0 CMOS Camera is easy to control with drivers that do not crash. The final choice landed on the Photron high speed camera as the overall performance was the best with large tuning possibilities of focal point and shutter opening, in the end of the project, stable drivers for the camera was acquired making it the logical choice.

### 4.5.1 Experimental Considerations

Many aspects have to be taken into consideration in obtaining the best possible visualization of the droplet experiments. The importance of triggering camera and light-source at the right time, alignment of laser-trigger and receiver and homogeneous droplets has been emphasized in previous sections. This part aims to highlight some of the challenges of recording droplets and describe counter measures. During the initial testing of high intensity laser and high speed camera triggering, the next picture was taken. The aim was to merely test if a droplet could successfully initiate image recording and minimal effort was made to produce data for further processing. However, the picture is in a neat way showing some of the most critical challenges related to image acquiring.

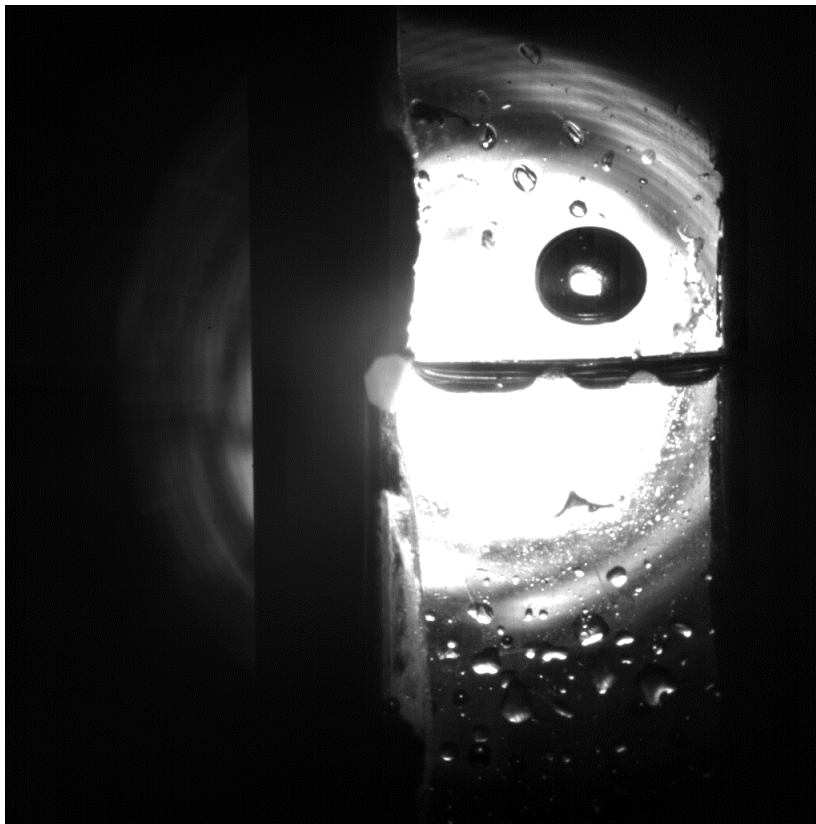


Figure 4.11: *A droplet of about 3 mm in diameter is approaching the interface in a visualization unit with a high power laser as a light source*

The first thing one might notice is the asymmetry of light concentrated to the right, as the resolution is adjustable it can be considered as an aesthetic issue. Still, the alignment of lights source, visualization unit and camera is important as the intensity of the light beam decrease radially. A clear circular focus area defined by the light beam emerges, by studying a series of pictures of a drop approaching the interface, it appears that the size of the droplet gradually decrease at it goes from dark, to gray and then to bright area. This

is off course not the case but the lack of light produce shadow effects on the droplet border making it to appear larger then what it is, this effect is reduced as it enters the focus region of the beam. In the opposite end of the scale, light intensity could be so strong that it completely wipes out the boarders making the droplet to appear as faded.

A very distinct phenomena is the appearance of a bright spot in the otherwise dark droplet caused by light passing directly through the object. When located in the center of the droplet it can easily be compensated by software-filtering, but the spot can wander as the droplet progress and making the boarder unclear. A similar issue is taking place after the droplet has reached the interface causing ripples in the water, the waves are reflecting light which is not unproblematic in respect of data processing.

A serious issue is the existence of liquid sticking to the inside of the visualization unit. Extraction and insertion of liquids and equipment cause water and oil to follow and stick to the wall in the opposing region of liquid. They cause reflections and hinder a direct view to the droplet, seriously deterring image quality. Attempts to clean the inside by inserting a brush or similar has proved to only make things worse and simply use time and wait does not cause the necessary effect. In this particular case the droplet is about 3 mm in diameter and the disturbances are for the most of the time not critical. Micro size droplets are about a 100 times smaller compared to the one present, and the surface area of the disturbing liquid is in many cases dominating a droplet on that scale. In the same manner it is apparent that the interface between oil and water is uneven. Water is creeping on the wall into the oil layer causing it to become bulgy. This is perhaps the most critical aspect as the study is based upon observation of coalescence. From preliminary studies no other solutions to these two problems other then cleaning and tweaking to the light-visualization unit and camera alignment were found, however it is valid expectation that applying high voltage to the system would induce electro coalescence and drastically reduce the problem. By charging the liquids not in contact with its homophase, they attract each other and coalesce to larger units, eventually joining the interface which is smoothen by being charged, as the liquid would seek to reduce the surface area to a minimum. By subsequently set the system in passive state by discharging, it could be performed as a standard procedure before each batch of experimental runs.

### 4.5.2 Image Calibration

Experiments using droplets of diameter about 3 mm was performed to calibrate the facility. All experiments used the same droplet size with constant signal to the camera and light source at 400 fps. At this rate a satisfactory amount of details and recording time was obtained. The camera used in the experiments is the Photron Fastcam SA3 high-speed camera as it shows the greatest potential and we could successfully recover drivers for automation. Finally, all experiments are recorded in the horizontal plane meaning that the camera is perpendicular to the interface which is the best position for software processing. By testing light sources and camera shutter opening the best interaction of light, visual-

ization unit and camera is found. First, the effect of shifting shutter opening for the high speed camera with white light on maximum power is studied.

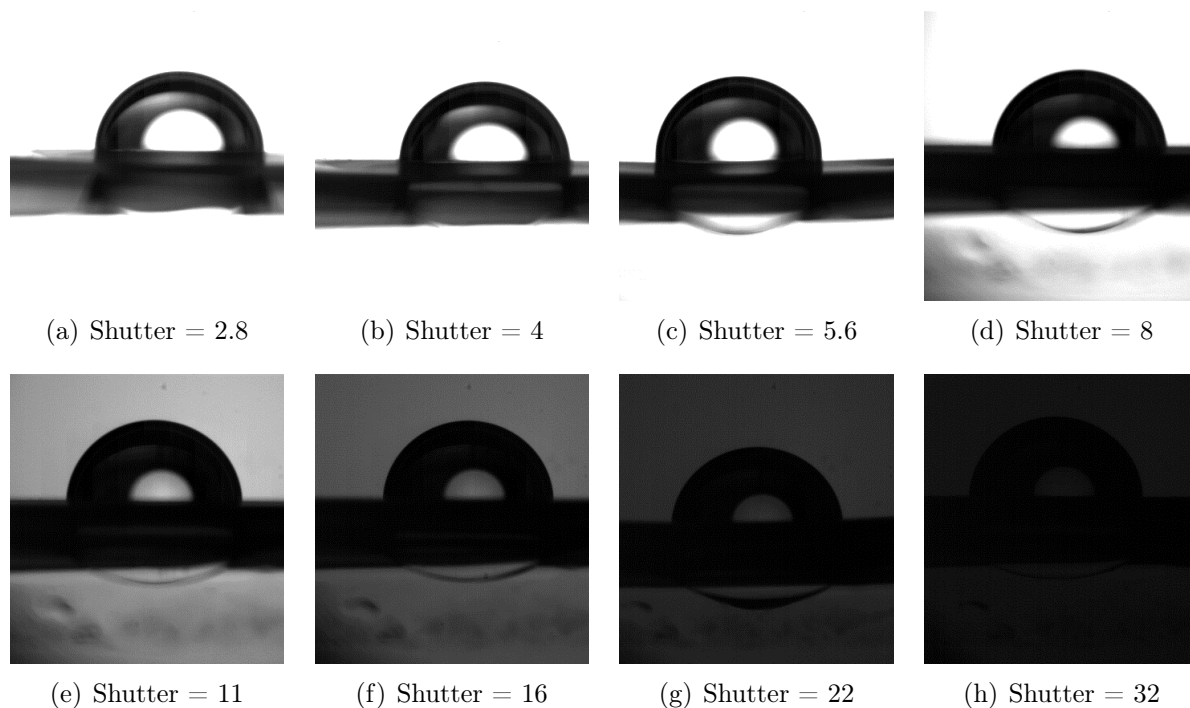


Figure 4.12: *A series of pictures showing the effect on image quality by adjusting the shutter opening. All settings but shutter opening are constant*

The sequence of images starts with maximum opening and ends with the minimum. A characteristic dark droplet with a white spot is resting on a dark interface, as the image becomes darker more and more information about the drop is appearing. Especially the submerged part of the drop becomes visible until the image goes completely dark. The downside is that the contrasts are decreasing, making it harder for a software to distinguish between droplet and the surrounding fluid. The images produced by shutter opening 2.8, 4 and 5.6 are the one best suited in analyzing coalescence time, they are missing some information, but have a high contrast. Each single image is of a unique droplet, in retrospect it would be much easier to just use one droplet and adjust the shutter of the camera on the way, but they do illustrate the high reproducibility of droplet shape, size and flow-path as they look very much the same.

As the preferred setting of shutter - light source was decided, the next step was to compare the two sources. The partial coalescence with white light on maximum power was captured by the camera with a shutter opening at 5.6. A droplet is resting on the interface and short after the coalescence is initiated, a few key images are chosen to show the coalescence and development of a daughter droplet.

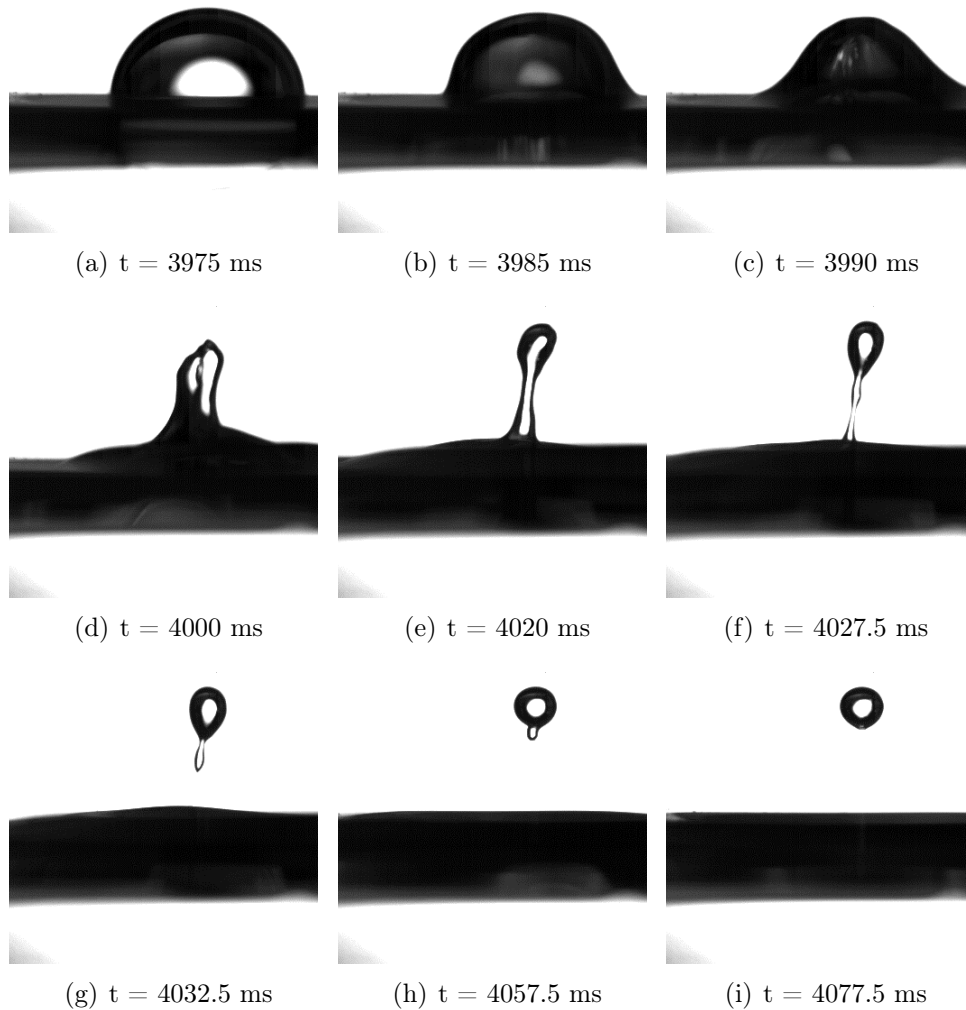


Figure 4.13: *Coalescence of a droplet visualized by white light*

Starting from top left, the droplet is resting on the interface and coalescence is initiated, as a part of the coalescence the droplet contracts and liquid exits from the center. The liquid quickly develops to a tip connected to the interface by a filament, by momentum and gravity forces thinning of the filament takes place and a erratic droplet detach from the interface. Due to surface tension the droplet develops to become spherical. The whole series of images shows a great contrast of droplet and interface to the surrounding fluid and is well suited for further processing.

The same analysis is done for the infrared light provided by the Oxford Firefly 300 W laser, in the control panel of the laser, duration is set to  $100 \mu s$  and the shutter opening of the camera is set to 16.

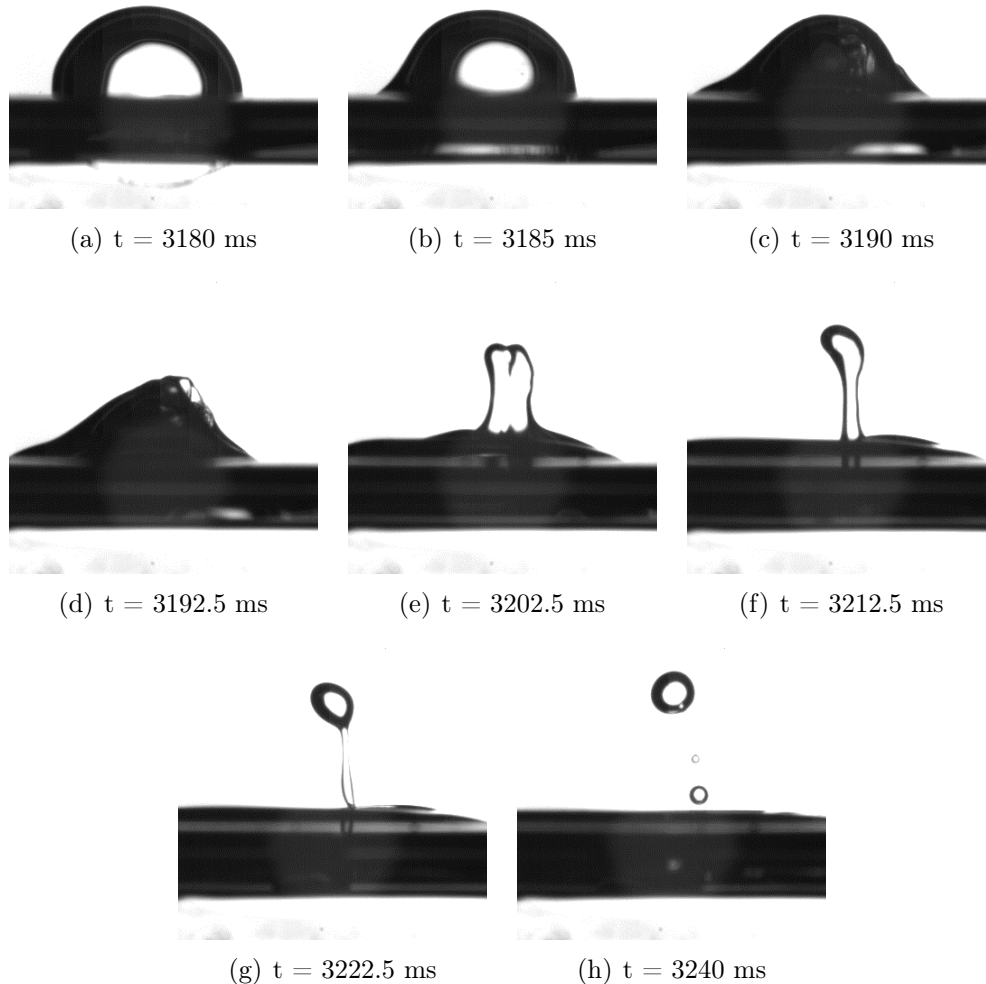


Figure 4.14: *Coalescence of a droplet visualized by infrared light*

The process of coalescence is the same as in the previous case of white light, the droplet rests on the interface and coalescence is initiated. The droplet contracts and liquid is ejected from the center, a tip connected to the interface by a filament is quickly formed. By gravity and momentum the filament is thinned until droplets are detached. It is very interesting to observe a total of three daughter droplets formed from the filament. The main droplet is substantially larger than the two others that most likely would have a different coalescence time due to size. Image quality is also very good in this case and in the end there are apparently no great difference in quality between the light sources. However, it is important to bear in mind that the tuning possibilities are much greater for the Oxford Firefly laser and the power can be substantially changed depending on the user preferences. The true quality of the laser, which is the ability to produce very short



and accurate pulses is not exploited to the full as the timespan of coalescence is too great. If e.g. the formation of a hole and initiation of coalescence is to be studied on a very detailed level, the attributes of the laser would come much more into play.

An interesting phenomena that occurs frequently is the partial coalescence of droplets, by studying the coalescence simply with the human eye it seems likely that the relative large droplet coalesces in a simple stage. This is seldom the case as witnessed by the previous image series of fig 4.13 and 4.14, here both 1 and 3 droplets respectively were formed from the liquid filament by the coalescence of the original droplet. A question rises, how many steps would it take before a droplet of this size is completely coalesced? To study this further the configuration of the camera is adjusted, the camera looks from above and down on the interface, tilted  $195^\circ$  to better see what is happening. In addition the resolution of the images are adjusted to obtain sufficient recording time. The next image series is of a droplet resting on the interface that partially coalesces in multiple steps.

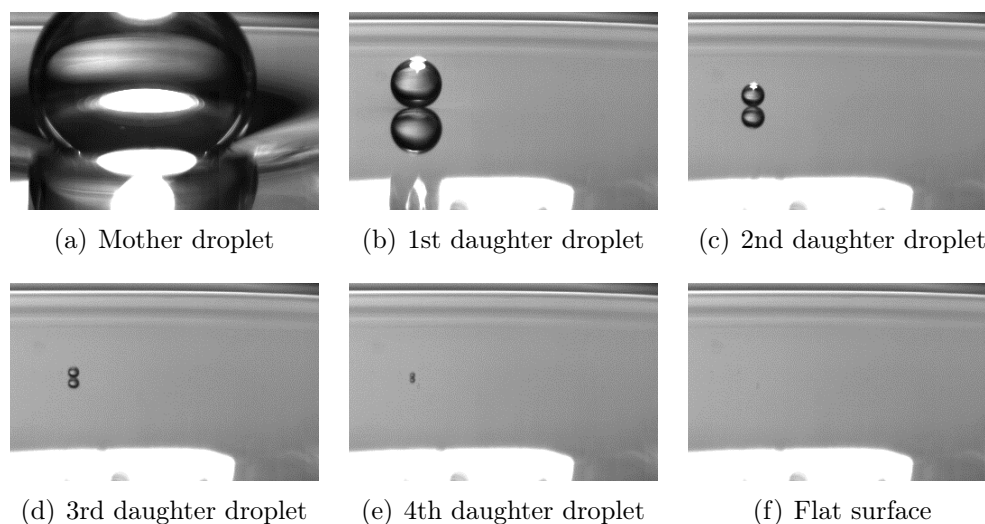


Figure 4.15: *Sequential images of partial coalescence in five steps, additional steps could be present but are not visible*

The initial mother droplet is too large to fit inside the frame, but we are able to see most of it and the contact with the interface. Coalescence is initiated, a liquid filament is ejected and a 1st daughter droplet is formed, resting on the interface. After some time the same happens to the 1st daughter droplet and a 2nd daughter droplet is formed. This pattern continues until a total of 4 daughter droplets are formed and coalesced in 5 steps. The partial coalescence is drastically reducing the resulting size of the new droplet and after the 4th daughter droplets has coalesced, no new droplet is visible. This doesn't mean that coalescence is completed, additional steps could take place but might be so fast and the droplet so small that they are not visible.

Something the reader might have noticed is the absence of disturbing liquid on the glass walls of the visualization unit. In section 4.5.1 this was highlighted as a critical

point of attention a long with the creeping interface. Somehow the liquid on the wall is not a substantial problem anymore, possibly this is due to the controlled execution of the experiments, but some of the answer is connected to the use of materials. The test unit described in fig 4.11 was of a steel tube with two extruded windows. The extrusion was made so two flat sheets of PVC could be inserted as windows to avoid bending of light. It seems that glass and PVC don't have the same challenges related to disturbing liquids and that contact angle and wetting ability of the surface might be the answer. In either case it is evident that by carefully insert and extract liquid to the glass visualization unit a lot of problems are avoided.

At the interface, the water phase tends to form a meniscus with a general higher level in the center then on the edges. It makes oil replace water close to the wall, but due to wall interaction the water level is not always constant and appears slightly bulgy, especially close to the corners of the visualization unit. By carefully adjusting the water level relative to the camera the effect of creeping liquid can be minimized. The aim should be to always place the droplets in the center with a free line of sight, especially micro size droplets that are very small, but implies low deformation to the interface.

Effort was made to keep the interface clean by frequently renewing it. Water/oil mixture was drawn from the interface by a needle and tap water was carefully replaced by a second needle to adjust the water level. After inserting a few droplets from the syringe, small objects always reappeared on the interface, it was discovered that the water tubing and syringe contained some sort of residue. Thin solid flakes were transported with the droplets and collected by the interface. This could affect coalescence time as bigger droplets have large attraction on the residue and contact would make a greater chance for coalescence. It is not clear if the residue comes from the water, tubing or both, but it is highly unwanted and should be treated.

## 4.6 Data Acquisition Chain and Automation

Fully automation of droplet generation, recording and processing would be a huge step in doing studies with a high amount of samples and low degree of uncertainties. Units that needs to be a part of such an automated system are the syringe pump, HV-generator, light source and camera.

National Instruments are the developer of a programed named LabWIEV (Laboratory Virtual Instrumentation Engineering Workbench) which is a platform design and development environment for visual programming. The graphical programming language used is named "G" and is a data flow language that execute events based on the structure of a graphical block diagram, especially suited for parallel execution and multiprocessing. Each LabWIEV program are called virtual instruments (VI) and consists of three components, a user GUI named front panel, a block diagram and a connector panel. By using the connector panel the block diagram of the current VI are represented in other VI's. The front panel support user input and extraction of data and is also useful in troubleshooting user developed programs.

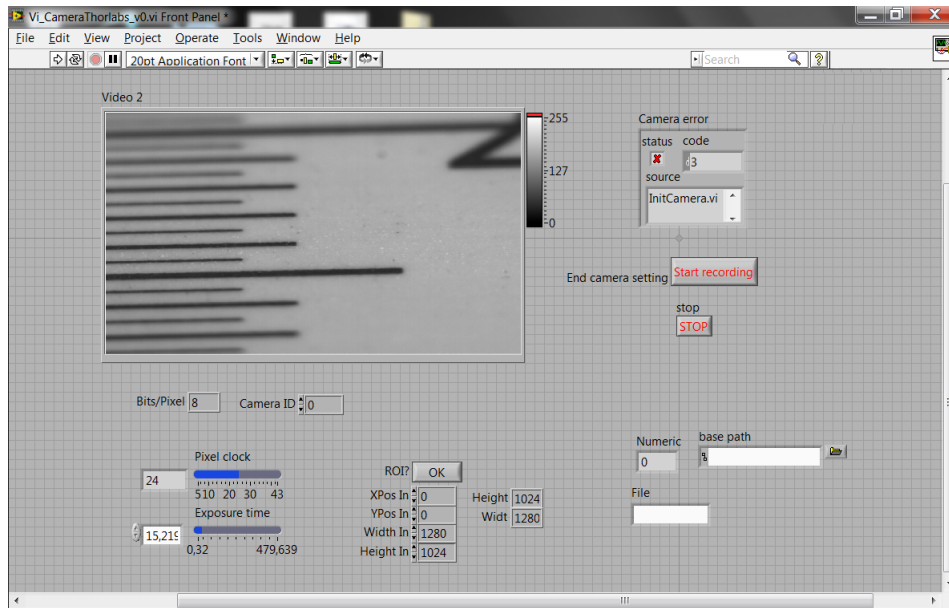


Figure 4.16: *The front panel with live stream and user input*

Next, the block diagram representing the front panel is shown with five main blocks, Initialization, initialization-process, Timeout, Main loop and End block. In the first block the camera is initialized by the user. Based on the camera ID, the acquiring of image and saving of data is initialized, if any errors occurs an error message is generated.

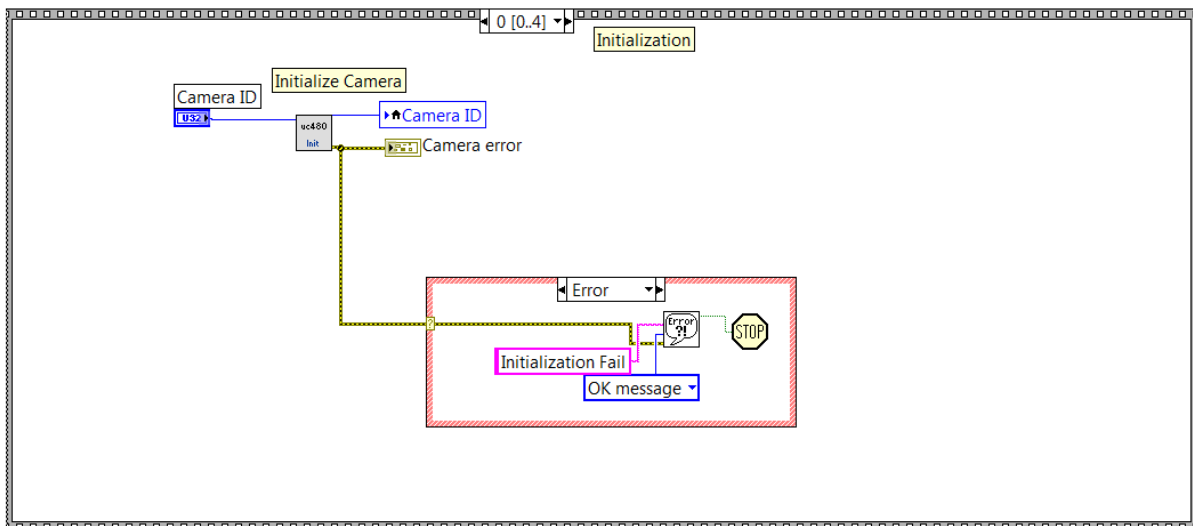


Figure 4.17: *Initialization of camera based on user input*

Based on user input, exposure time, image size and color depth is stepwise acquired and necessary memory is allocated.

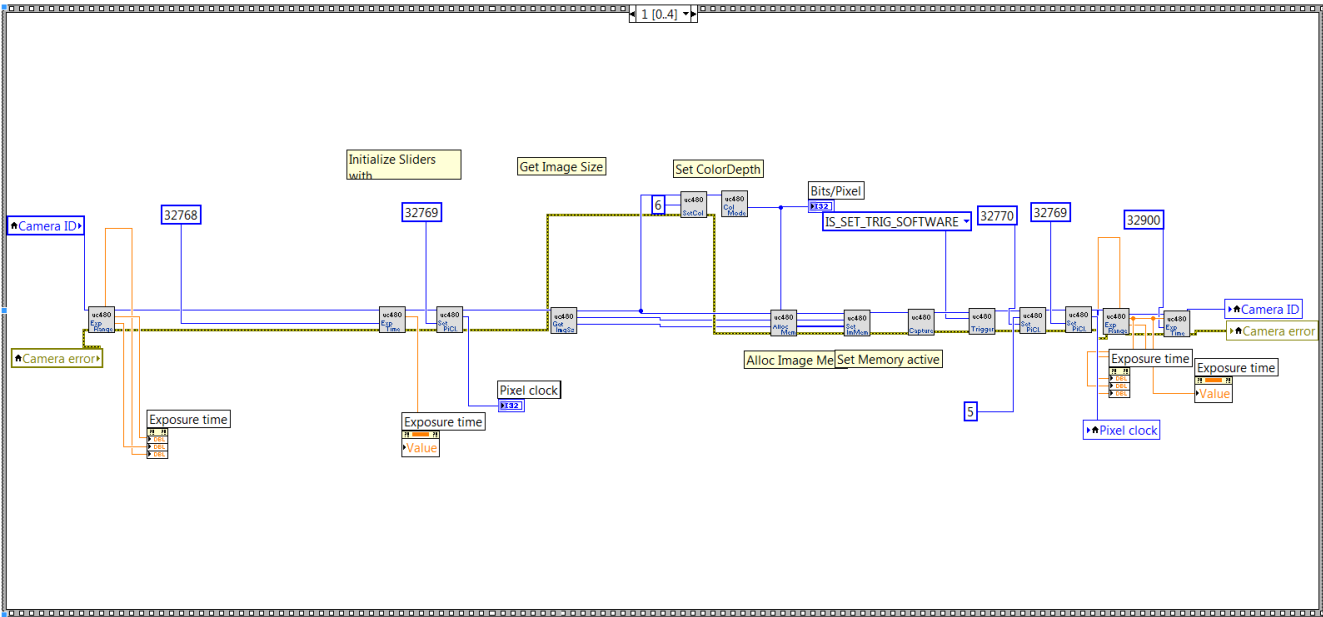


Figure 4.18: Initialization and allocation of memory

A live feed is now served the camera and video recording and data saving can be performed by the main loop. Two cases are presented in the image below, the top case includes a lot of desirable features in a complete experimental setup, but no code or operations are included. Instead, a simplified case is presented below focused on video recording and data saving. The simplified case is presented to give a better understanding of LabWIEV and can be extended to the more advanced case if the correct equipments and drivers are by hand.

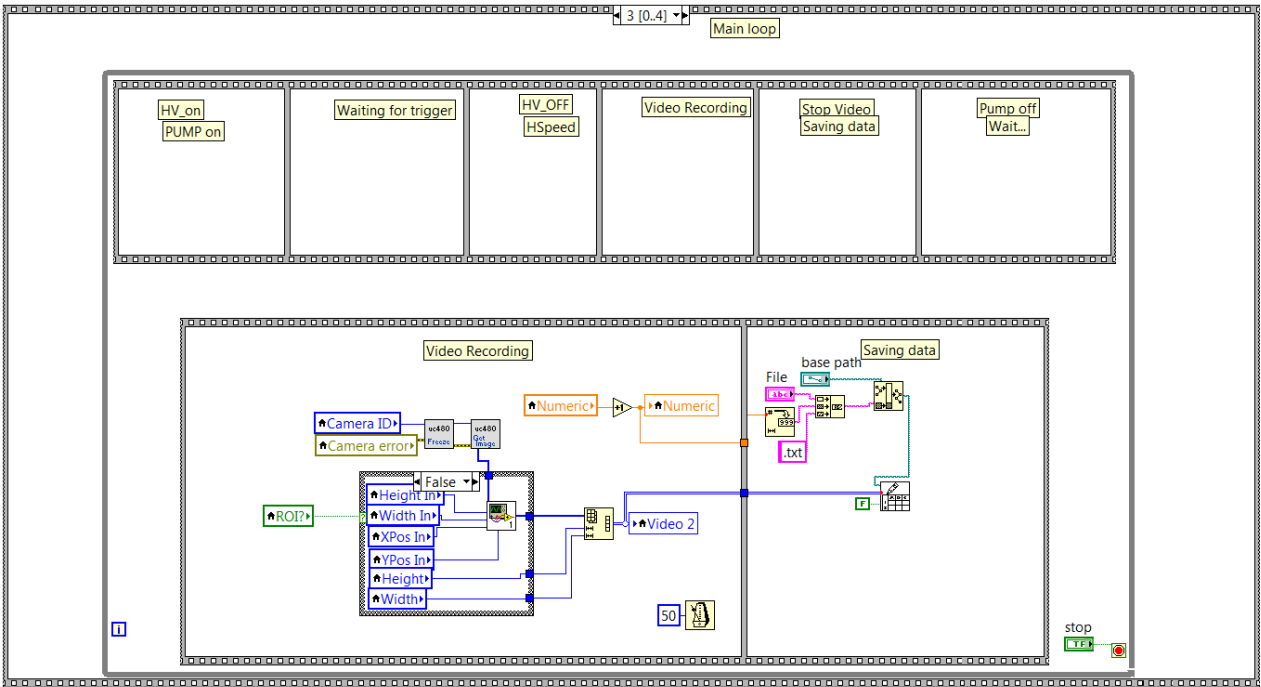


Figure 4.19: The main loop organizing the events taking place, in this case Video Recording and Saving data

Finally, the whole process is ended by a "stop capture" block, it is worth noticing that several sub-blocks are present in such a program but only the most important one to describe the structure are presented here.

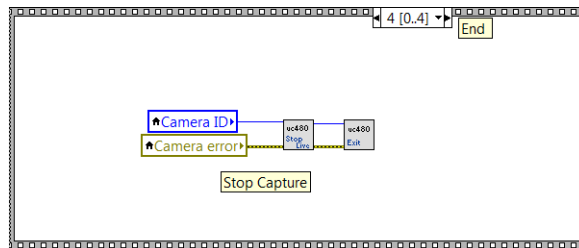


Figure 4.20: The end block terminating video recording

#### 4.6.1 Post Processing

The idea of a complete and fully operation facility is to capture experiments by a camera and then process images to obtain the experimental results. The droplet approach, impact and coalescence are captured by the high speed camera at a given frame rate. The rate must provide a satisfying amount of information, combined with adequate recording capacity.

Each sequence contains as many as 10.000 frames or more and illustrates the amount of information available. In similar processing of pictures from the high-speed camera, a commercial software named VisiSize is used in addition to extensive manual work. VisiSize loads a batch of frames and identifies the number of objects, roundness and the diameter of the droplets in each frame. Velocities and coalescence time must then manually be calculated, alternatively all of the information can be obtained by visually examine the frames in MATLAB and measure - by hand the parameters of interest. This is a even more time consuming process which gives little consistency with regards to the point where the diameter is calculated, border of the droplet and velocity calculations and hence a source for errors. Some work is done to make a routine that analyses the recorded images, but more work is needed to complete the task.

By every experiment, a sub folder containing the frames for each droplet is automatically created. Organizing like this makes it easy to distinguish between each individual droplet. A routine is pointed to the parent folder and takes in every sub folder, one at a time. After entering a sub folder every frame is processed by the script. A gray scale image is imported to MATLAB, a threshold between 0 - white to 255 - black is identified, and is applied to the gray scale image. The result is a black and white image where the borders of a droplet or other objects casting a shadow are clearly defined. Due to reflection of light, objects in the image might have white areas where the level of black were less than the threshold level, these areas are filled as a step in filtering the picture for background noise and unwanted objects, like satellite droplets or dust. Objects in the image, including the background noise, interface and droplet are now appearing as solid black. As a final step the whole image is reversed, the final image should contain only the white droplet and interface on a black background, ready for data measurements.

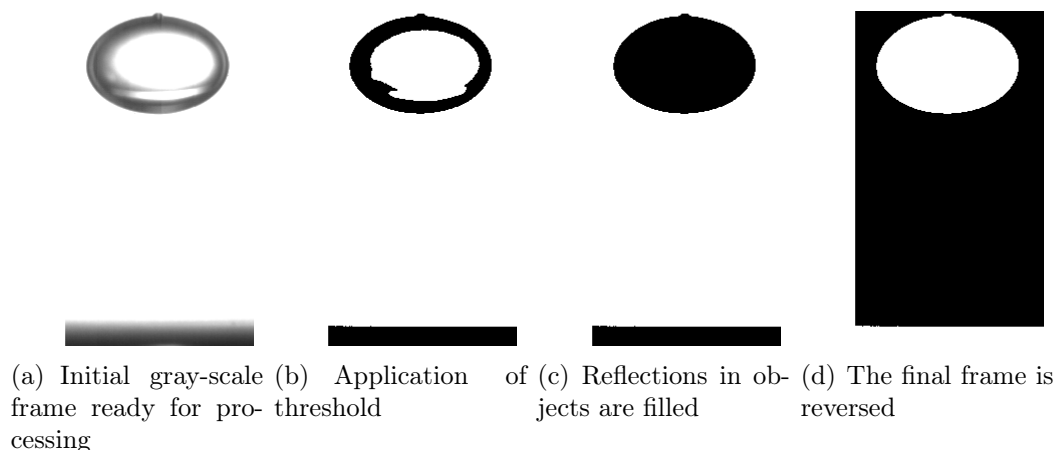


Figure 4.21: *The process of manipulating raw-data where relevant parameters can be extracted*

The parameters of interest can now be extracted from the final image. Object area, perimeter, major and minor axis are calculated for both the droplet and interface while

the droplet is identified by its "roundness". The roundness describes how close the shape of an object is to a perfect circle and naturally the droplet is more circular than the interface.

The next step is to identify the position of the droplet in the image and measure velocity and coalescence time. Possibly a routine can be used to search through every row until the white droplet or interface are identified. Velocity is calculated by using the frame rate, pixel-width and droplet displacement between the frames. In principle, coalescence can be identified by a droplet merging with the interface, leaving it flat. The coalescence event of a droplet with a size of millimeters in diameter is generating a lot of motion making it hard to identify the event by a still surface. It is expected that droplets of micrometers will perform much better, but this is still an issue that is not completely solved.

## 4.6.2 Drop Size Measurement

The equivalent diameter to a perfect sphere is calculated on the basis of the major and minor axis. A perfect sphere deformed between two parallel plates will get the shape of an oblate spheroid. It can be perceived as a compressed sphere consisting of one minor axis and two major axes of the same length. By rotating a circle around its own axis a perfect sphere is obtained, by rotating an ellipse you obtain an oblate spheroid.

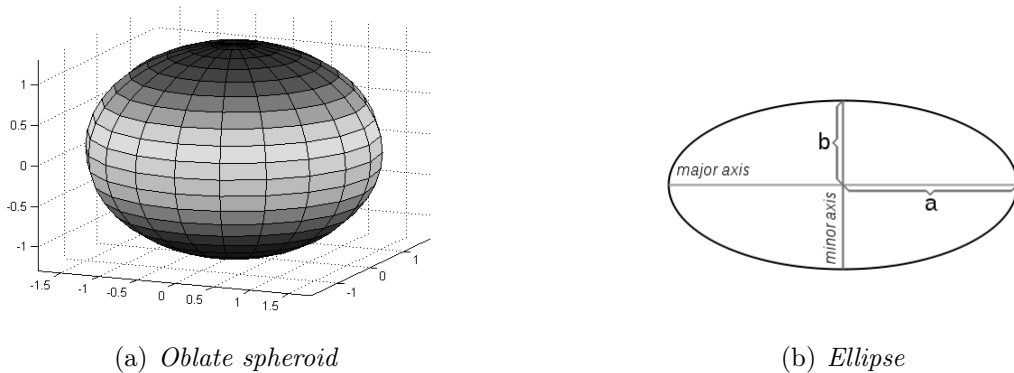


Figure 4.22: Length scale of a compressed drop,  $a$  is major and  $b$  is minor axis

The equivalent diameter of the oblate spheroid to a perfect sphere is calculated by considering the droplet volume. It is assumed that the droplet is incompressible and the volume constant. By considering the two volumes the equivalent radius and diameter are obtained.

$$V = \frac{4}{3}\pi r^3 = \frac{4}{3}\pi a^2 b \quad (4.1)$$

$$d = 2r = 2(a^2 b)^{\frac{1}{3}} \quad (4.2)$$

The equivalent spherical diameter can be used to describe the droplet size in the experiments. If the major and minor axis are equal the droplet is shaped as a perfect sphere.

## 4.7 Facility

The assembled facility is made up by all the subunits, modules and processes described so far in this chapter. Interaction of the parts and other equipment is presented in this section. Several events are executed simultaneously or slightly delayed when a droplet is recorded, interaction of multiple devices based on a pulse signal generated by the droplet is illustrated in a flow chart below.

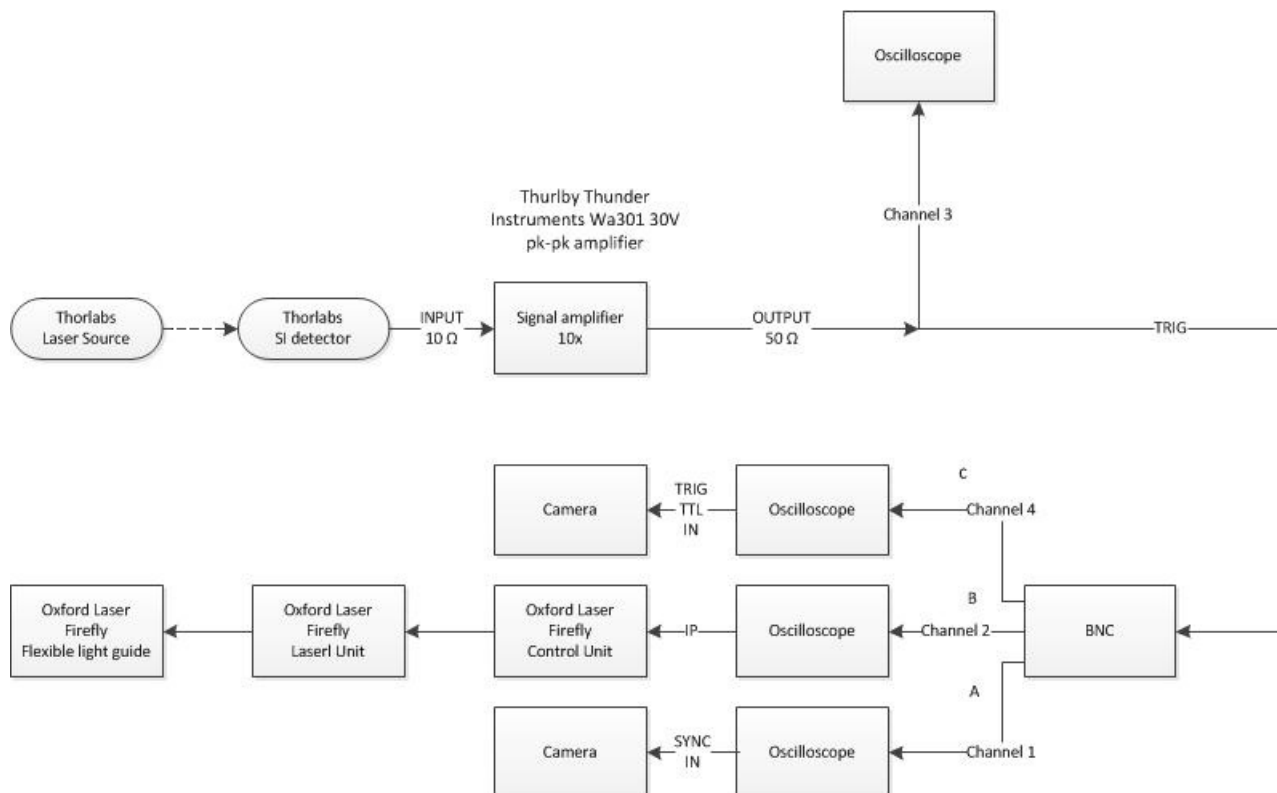


Figure 4.23: *The path of a droplet generated signal*

A continuous laser beam is emitted from a Thorlabs S1FC635 Fiber Coupled Laser Source, the beam is traveling through the cage and glass container filled with oil and is collected by a Thorlabs SI detector. When a droplet is intersecting the laser beam, a signal is produced and amplified 10 times by a Thurlby Thunder Instruments Wa301 30V pk-pk amplifier. The amplified signal is then directed to the BNC 575 delayer / pulse generator. An oscilloscope is applied to visualize the signal after amplification, in this way it helps understanding the process and is perfect for signal verification. The main task to the BNC is to subsequently trigger light source and camera recording, additionally it is used to control frame rate and pulse shape. Three unique signals are sent from three different BNC ports, two to the camera and the last to the light source making it possible to trigger them independently. The output signals are visualized by the oscilloscope.



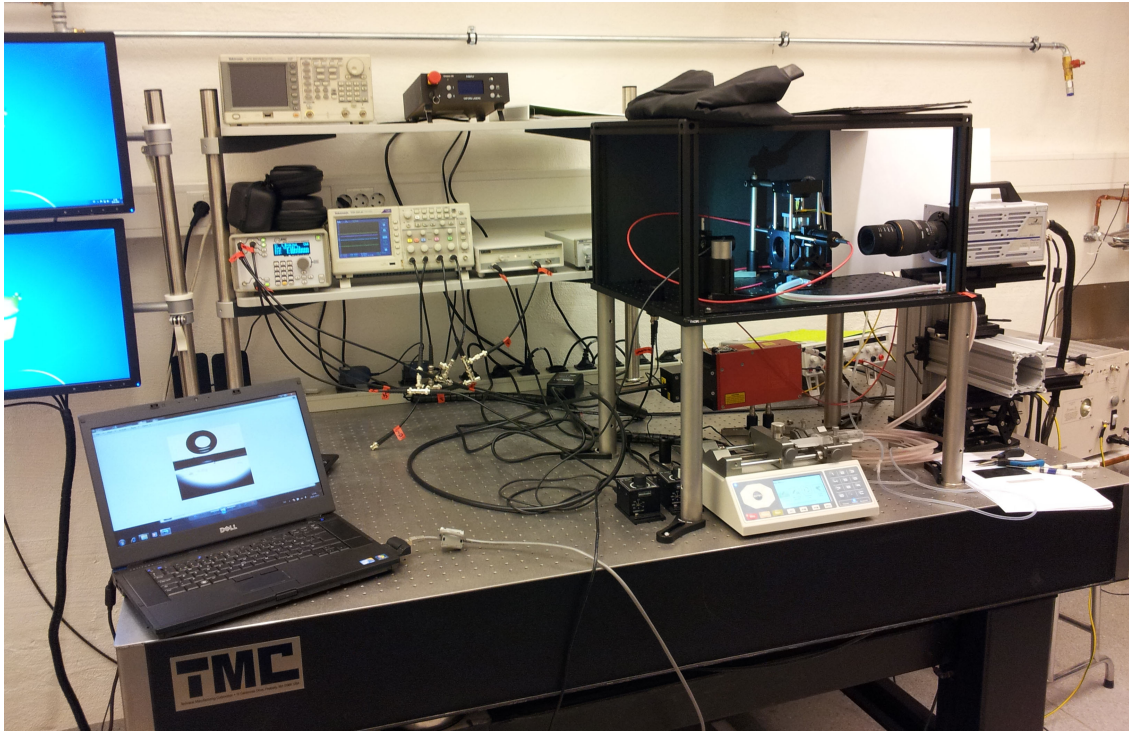


Figure 4.24: *Complete experimental setup, to the left is a laptop and two screens for a stationary computer, in the back is all the signal treatment equipment and high intensity laser placed on a shelf. The visualization unit with trigger, light source and camera are placed within the enclosure that is open for the moment. All the way to the right, the high voltage unit can be spotted located on a table*

Droplets of uniform size are produced by a Nexus 3000 syringe pump at a low infusion rate  $\sim 0.01$  ml/min in close cooperation with a 5kV Trek 5/80 High-Voltage Power Amplifier. A hose is connected from the syringe to a needle of diameter depending on the desired meniscus size. By applying voltage pulses to the meniscus, micro size droplets of uniform size are produced.

The droplet-interface interaction is captured by a Photron Fastcam SA3 high-speed camera with ability of shooting 1024 x 1024 pixel resolution at a frame rate of 1,000 fps to a reduced resolution and frame rate of 60,000 fps. The lens used is a Sigma 105 mm, 1:2,8D DG Macro unit with a distance between the lens and camera to the visualization unit at about 15cm.

Lighting is provided by a Thorlabs MCWHL2 LED lamp, giving cold white light or a Oxford Firefly 300 W laser. The LED light source is powered by a Thorlabs Led-Driver, LEDD1B 0-1200 mA, set to maximum. Both light source gives very concentrated light at a narrow wavelength which in turn is filtered by a diffuser provided a long with high power laser to better visualize the shadow casting of the droplet, the light is positioned just next to the column.

The high-speed camera is triggered by the droplet detection mechanism. A Thorlabs S1FC635 Fiber Coupled Laser Source is attached with a fiber-optic cable pointed to a CVH100-COL Thorlabs Fiber Adapter with Lens Mount and directed by a second fiber-optic cable to a Thorlabs SI Biased Detector. Thickness and spreading of the laser beam is controlled by a Thorlabs LB1761 BI-Convex lens with focal distance  $f=25,4$  mm and a lever-actuated iris diaphragm for governing the beam size, set to the minimum opening. Travel distance of the free laser beam is about 18 cm with the visualization unit in between. The laser beam intersects the fluid column and all disturbances to the beam are registered by the detector. When a droplet intersects the laser beam an electric pulse is sent to a Thurlby Thunder Instruments Wa301 30V pk-pk amplifier to meet the camera trigger requirement of 1 - 5V. Laser and detector are rigidly align by using a Thorlabs cage system and parts described in section 4.2.

From the amplifier the signal is sent to a BNC Model 575 Digital Delay / Pulse Generator, the time delay and signal width is set by the user. From the delayer a 1-5 V step pulse is produced and triggers the high-speed camera.

To avoid being in the dark, a Tektronix TDS 2014C four channel digital oscilloscope is added to visualize signals in different parts of the pulse processing. Signals before and after the amplifier, from the BNC to the camera and from the BNC to the light source are sent to the oscilloscope.

# Chapter 5

## Conclusion and Recommendation

### 5.1 Conclusion

The focus of this thesis was to analyze, plan, order, develop, execute and build a facility for droplet - interface coalescence. The main aspects of that process was described in detail in the Result and Discussion chapter and those main points are reviewed here.

The facility is designed to generate droplets with size from 50 microns to 1.000 microns. The broad specter of sizes are covered by two generation methods, the largest droplets are generated by using a syringe pump with needles of different diameters. Generation is easy and the size is directly related to orifice size. For the rest of the droplet-sizes the generation is done by a high voltage amplifier, unfortunately the machine malfunctioned due to a factory defect and is returned to the supplier for service and repair. As soon as the amplifier is back in working condition, testing can start on the smallest droplets as the rest of the equipment to do so are in place.

The benefit of droplet detection and importance of perfect alignment of laser and detector was stressed during development of the detection unit. It is used for automate illumination and high speed visualization of the droplet interface coalescence to reduce, manual work and exposure to potential hazardous radiation from the high power laser. By a combination of a adjustable driver, iris and a lens the thickness and sensitivity of the laser beam is adapted to the droplet size, it works well for the largest droplets and by the obtained sensitivity it is assumed that it could handle the smallest droplets as well.

Two sources for illumination are used in the facility, a easily controllable Thorlabs MCWHL2 LED lamp emitting white light is a flexible source easy to mount and the preferred source for adjusting and testing the facility. The other is the Oxford Firefly 300 W laser, it is very powerful and ideal to illuminate fast processes as the source produce very short and accurate pulses. The light emitted is infrared and can be potentially hazardous even by indirect viewing, hence rigid safety measurements are taken to reduce the risk and is the reason white light is the preferred source for testing. Two liquid systems, water and Exxsol D80 and water and petroleum were tested, the system containing petroleum was tested with the infrared light, but the wavelengths did not match the petroleum and were

not able to shine through small layers of liquid. The combination of water and Exxsol D80 is successfully illuminated by both sources, the reason for also evaluating petroleum was the appealing thought of studying water oil systems directly.

Not only the light source is important in visualization of the experiments, but close cooperation between light, visualization unit and camera is needed to obtain the best images possible. For this purpose the visualization unit was developed, in this module the droplets are released from a needle and travels through a oil phase before it settles and coalesces on the water interface. To reduce bending of light the walls are straight instead of curved and are custom made by a glass workshop to match the dimensions of the detection module and rest of the facility. Liquids can easily be removed or added by removing the lid on top of the unit, integrated in the lid is a conductive needle connected to a high voltage amplifier by a wire, the matching electrode is integrated to the base, directly in contact with the water phase and connected to the high power amplifier output by a wire. The needle and electrode are connected to the high power amplifier in order to generate the smallest droplets, even though the generation was not tested the unit is build to accept them. To capture the coalescence, a Photron high speed camera was applied due to it's superior frame rate and adjusting possibilities for focal point and shutter. By applying pulsed light with the same frequency and shape as camera frame rate, the images obtained where of high quality, ready for processing.

Size controllable droplets are produced and can trigger the light and recording of the coalescence process. By using LabVIEW it is possible to obtain full automation of droplet generation, recording and storage. Drivers to the high speed camera and syringe pump have been acquired and are the basis of automating large droplets study. The system can be extended when the high voltage amplifier is repaired to include small droplets. The last step in completing a fully automated facility is the post processing, images are loaded to MATLAB and by extensive manipulation the interesting parameters as size, terminal velocity and coalescence time are extracted. Large droplets induces a lot of fluid motion when coalescing, complicating the software detection of coalescence. This can be worked around and it is believed that it would be less of a problem with small droplets due to size.

By the observations that are done during facility building and testing it can be concluded that droplets seldom coalesces in a simple stage. With the size of  $\text{Ø}3$  mm it is observed coalescence in as many as five steps and there is a sense that the cascade of droplets includes even more steps, but are too small or fast to be captured with the settings for this study.

## 5.2 Recommendation

The main point in further work should be to finalize the automation of the facility in labVIEW and to complete the post processing by deciding a decision criteria for coalescence time. With this in place, automated experiments of droplets produced by needles and a syringe pump can be done and proper statistical evaluations can be made in this size range. When the high voltage amplifier returns, testing can be done and the same process of making a statistical evaluation can be applied to micro size range as well.

A developed model of the visualization unit is made in this thesis, it allows for fluid circulation as controlling temperature gradients is important in coalescence. Besides the minor modification of the base made of a single piece with an electrode of stainless steel, renewing of the interface through the circulation point could be interesting. It was found that the syringe and hose contained some form of residue which needs to be eliminated maybe by distilling water before use, but renewing of the interface could be an aid of avoiding similar issues. An alternative design not described in the thesis could be to make a unit where the top part matches the laser detection module while the bottom part is much wider, containing the interface. By increasing the dimensions in the bottom, wall effects can be reduced and the making of a leak-proof removable base would become easier while the important triggering mechanism works as before.

Increasing recording time and frame rate of the high speed camera is something to consider if it is desired to study the coalescence even closer, although the current settings of 400 fps are sufficient for recording the partial coalescence of a droplet in five steps, not calling for further upgrades at this stage. If an upgrade of the camera should turn out to be interesting it costs about 5,500 EUR to replace the 2 GB internal memory with 8 GB according to the supplier. The unit must be shipped to the UK and replacement is completed within 2 days which is quite fast, allowing such an decision to be made when it is found needed without seriously delaying the whole project.

Adding one or two amplifiers to ensure signal triggering even by the smallest droplets and to make the facility more robust is something easily done. Similarly adding an acquisition board to ease the handling of signals and automation should be seriously discussed, it is not a big investment but requires some work. The stock light diffuser following the high power laser is used for both light sources and drastically increase the image quality by allowing stronger light giving a homogeneous background light. The diffuser is quite dark, filtering a lot of light and it could be useful to see if less dark filters are performing better.



# Bibliography

- [Basheva, 1999] Elka S. Basheva, Theodor D. Gurkov, Ivan B. Ivanov, Grigor B. Bantchev, Bruce Campbell and Rajendra P. Borwankar *Size Dependence of the Stability of Emulsion Drops Pressed against a Large Interface*. Langmuir, Volume 15, Issue 20, 1999, Pages 6764-6769
- [Traykov, Ivanov, 1977] T.T. Traykov, I.B. Ivanov *Hydrodynamics of thin liquid films*. International Journal of Multiphase Flow, Volume 3, Issue 5, August 1977, Pages 471-483
- [O. Reynolds, 1886] O. Reynolds 1886 *On the Theory of Lubrication and Its Application to Mr. Beauchamp Tower's Experiments, Including an Experimental Determination of the Viscosity of Olive Oil*. Phil. Trans. R. Soc. Lond. Issue 177, 1886, Pages 157-234
- [Charles and Mason, 1960] G. E. Charles and S. G. Mason *The coalescence of liquid drops with flat liquid/liquid interfaces*. Journal of Colloid Science 15, 1977, Pages 471-483
- [Vrij, 1966] A. Vrij *Possible Mechanism for the Spontaneous Rupture of Thin, Free Liquid Films*. Discussions of the Faraday Society Volume 42, 1966, Pages 23-33
- [A. Dupre, 1869] A. Dupre *Théorie Mécanique de la Chaleur*. 1869, Paris
- [M. Dhainaut, 2002] M. Dhainaut *Literature Study on Observations and Experiments on Coalescence and Breakup of Bubbles and Drops*. NTNU, 2002
- [Janssen, 1993] J. M. H. Janssen and H. E. H. Meijer *Droplet breakup mechanisms: Stepwise equilibrium versus transient dispersion*. Centre for Polymers and Composites, Eindhoven University of Technology, 1993 URL: <http://alexandria.tue.nl/repository/freearticles/586294.pdf>
- [Grace, 1971] Grace, H. P *Dispersion phenomena in high viscosity immiscible fluid systems and application of static mixers as dispersion devices in such systems*. Chemical Engineering Communications, Volume 14, 1982, Pages 225-277
- [Taylor, 1934] G. I. Taylor *The Formation of Emulsions in Definable Fields of Flow*. Proceedings of the Royal Society of London. Series A, Volume 146, 1934, Pages 501-523 URL: <http://www.jstor.org/stable/2935605>

- [Stewart, 2008] Maurice and Stewart *Gas-Liquid And Liquid-Liquid Separators*. Gulf Professional Publishing Chapter 4, 2008, Pages 131-174 URL: <http://www.sciencedirect.com/science/article/pii/B9780750689793000040>
- [Mokhatab, 2006] Saeid Mokhatab, William A. Poe and James G. Speight *Handbook of Natural Gas Transmission and Processing*. Gulf Professional Publishing Chapter 4, 2006, Pages 197-246 URL: <http://www.sciencedirect.com/science/article/pii/B9780750677769500105>
- [Cusack, 2009] R. Cusack *Rethink your liquid-liquid separations*. Hydrocarbon Processing June 2009 Pages 53-60 URL: <http://www.koch-glitsch.com/Document>
- [Langl and Wilke, 1971] Sidney B. Langl and C, R. Wilke *A Hydrodynamic Mechanism for the Coalescence of Liquid Drops. I. Theory of Coalescence at a Planar Interface*. Ind. Eng. Chem. Fundamen. August 1971, Volume 10 (3) Pages 329–340 URL:<http://pubs.acs.org/doi/pdf/10.1021/i160039a001>
- [Langl and Wilke, 1971] Sidney B. Langl and C, R. Wilke *A Hydrodynamic Mechanism for the Coalescence of Liquid Drops. II. Experimental Studies*. Ind. Eng. Chem. Fundamen. August 1971, Volume 10 (3) Pages 341–352 URL: <http://pubs.acs.org/doi/pdf/10.1021/i160039a002>
- [Lawrence, Nielsen and Adams, 1958] Lawrence E. Nielsen, Robert Wall and George Adams *Coalescence of liquid drops at oil-water interfaces*. J. Colloid Sci. March 1958, Volume 13 Pages 441-458
- [Pearson, 1916] Karl Pearson *Mathematical Contributions to the Theory of Evolution. XIX. Second Supplement to a Memoir on Skew Variation*. Philosophical Transactions of the Royal Society of London. Series A 1916, Vol. 216 pp. 429-457 URL: <http://www.jstor.org/stable/91092>
- [Tsukatan and Shigemitsu, 1980] Tsuneo Tsukatani, Kazuyuki Shigemitsu *Simplified Pearson distributions applied to air pollutant concentration*. Atmospheric Environmen Volume 14, Issue 2, 1980 Pages 245-253 URL:<http://www.sciencedirect.com/science/article/pii/000469818090284X>
- [SSB, 2010] SSB *Produksjon og reserver, 4. kvartal 2010*. Issue 4, 2010 URL:<http://www.ssb.no/ogprodre/arkiv/tab-2011-02-25-01.html>
- [Perry, 1950] Perry, J. H., Ed., *Chemical Engineers Handbook*. 3rd. ed., 1950 McGraw Hill company, inc.
- [Wright et al. 1993] G.S. Wright, P.T. Krein and JC. Chato *Self-Consistent Modeling of the Electrohydrodynamics of a conductive Meniscus*. Conf. Rec. 1993 IEEE-IAS Annual Meeting, 93CH3366-2, pp. 1946-1955.



- [Atten et al. 2008] P. Atten, A. Ouiguini, J. Raisin and J.-L. Reboud *Drop-on-demand Extraction from a Water Meniscus by a High Field Pulse*. IEEE International Conference on Dielectric Liquids (ICDL-2008), Poitiers, June 30-July 4, 2008 URL:<http://hal.inria.fr/docs/00/37/20/95/PDF/Atten-1-ICDL08.pdf>
- [Raisin, 2011] J. Raisin, *Electrocoalescence in water-in-oil emulsions: towards an efficiency criterion*. PHD report, April 8th, 2011, University of Grenoble, France.
- [Kassim and Longmire, 2004] Zulfaa Mohamed-Kassim, Ellen K Longmire *Drop coalescence through a liquid/liquid interface*. American Institute of Physics, 2004 Volume: 16, Issue: 7, Pages: 2170
- [Gillespie and Rideal, 1956] Gillespie, T. and Rideal, Eric K., *The coalescence of drops at an oil-water interface* The Royal Society of Chemistry, 1956 Trans. Faraday Soc., vol.52, pages 173-183 URL: <http://dx.doi.org/10.1039/TF9565200173>

# Appendix A

## 'getAllFiles'

```
function fileList = getAllFiles(dirName)
dirData = dir(dirName); % Get the data for the current directory
dirIndex = [dirData.isdir]; % Find the index for directories
fileList = {dirData( dirIndex).name}'; %' Get a list of the files
if isempty(fileList)
    fileList = cellfun(@(x) fullfile(dirName,x),... %Prepend path to files
        fileList,'UniformOutput',false);
end
subDirs = {dirData(dirIndex).name}'; % Get a list of the subdirectories
validIndex = ismember(subDirs,{'.','..' '.db'}); % Find index of subdirectories
% that are not '.' or '..'
for iDir = find(validIndex) % Loop over valid subdirectories
    nextDir = fullfile(dirName,subDirs{iDir}); % Get the subdirectory path
    fileList = [fileList; getAllFiles(nextDir)]; % Recursively call getAllFiles
end
end
```

# Appendix B

## 'removeThumbs'

```
aa=cell(0)
a=getAllFiles('folder1')
a
c=1;
for i=1:length(a)
    if (strfind(a{i}, 'Thumbs') >0)
        else
            aa{c}=a{i};
            c=c +1 ;
        end
    end
end

for i=1:length(aa)
    aa{i}
end
```

# Appendix C

## 'imgProc'

```
function output = imgProc(imageList)

num_images = size(imageList)

% Get the folder name, which is stored in the last cell.
folderName = imageList{num_images}

for k = 1 : num_images % Analyze all images...

    filename = fullfile(imageList{k})
    % Check to see if it really exists.

    % Image exists!
    % Read it in.
    gray = imread(filename);

    % Read in the image.
    % gray = imread(fileName);

    grayAdj = imadjust(gray);
    level = graythresh(grayAdj); % Apply treshold
    blackWhite = im2bw(grayAdj,level);

    %ignoring all white openings with an area less then 6000 pixels
    %like small droplets or reflection (bw - BlackWhite)
```

```

blackWhiteAdj = bwareaopen(blackWhite, 6000);

% reverse the image from a black to a white drop to be able to further
% process it
revImg = blackWhiteAdj < max(blackWhiteAdj(:));

% removes disturbances in the picture like dust or glare. Are used instead
% of the - imopen command
finalImg = bwareaopen(revImg, 1000);

K(1:512)=0.5;
M=(1:1:512);

column50=finalImg(:,50);
column75=finalImg(:,75);
column100=finalImg(:,100);
column125=finalImg(:,125);
column150=finalImg(:,150);

pos50=intersections(M,column50,M,K);
pos75=intersections(M,column75,M,K);
pos100=intersections(M,column100,M,K);
pos125=intersections(M,column125,M,K);
pos150=intersections(M,column150,M,K);

dropPoint=min([pos50' pos75' pos100' pos125' pos150']);

if(any(dropPoint==pos50))
    coord=[50,dropPoint];
    xcoord=coord(1);
    freeDrop=length(pos50');
end

if(any(dropPoint==pos75))
    coord=[75,dropPoint];
    xcoord=coord(1);
    freeDrop=length(pos75');
end

```

```

if(any(dropPoint==pos100))
coord=[100,dropPoint];
xcoord=coord(1);
freeDrop=length(pos100');
end

```

```

if(any(dropPoint==pos125))
coord=[125,dropPoint];
xcoord=coord(1);
freeDrop=length(pos125');
end

```

```

if(any(dropPoint==pos150))
coord=[150,dropPoint];
xcoord=coord(1);
freeDrop=length(pos150');
end

```

```

figure(9)
subplot(1,2,1)
spy(finalImg);

```

*% % % Shows the colour ditribution along a given column*

```

figure(10)
subplot(1,2,1)
plot(finalImg(:,100),'b-')
subplot(1,2,2)
plot(finalImg(:,150),'b-')

```

*%identifies the interfase level at row one(1) and levels it to this hight*

```

I=find(finalImg(:,1)== 1);
finalImg_new=finalImg;
finalImg_new(I(1):end,:) = 1;

```

```

figure(9)
subplot(1,2,2)
spy(finalImg_new);

```

*%%%identify the most round object (help roundness)%%%*

```

% identify the boundaries in the image
[B,L] = bwboundaries(finalImg_new);

```

```

% calculates object properties like diameters and surface area
data = regionprops(L,'all','Centroid');

strInd= strfind(filename,'C001H001S0001');
timeFrame=str2num(filename(strInd+13:strInd+13+5));

% loop over the boundaries
for l = 1:length(B)

metric(l)=0;
% obtain (X,Y) boundary coordinates corresponding to label 'l'
boundary = B{l};

% compute a simple estimate of the object's perimeter
% delta_sq = diff(boundary).^2;
% perimeter = sum(sqrt(sum(delta_sq,2)))
perimeter = data(l). Perimeter;

% obtain the area calculation corresponding to label 'l'
area = data(l).Area;

% compute the roundness metric
metric(l) = 4*pi*area/perimeter^2;

% stores the diameter of the roundest object
d1(l) = data(l). MajorAxisLength;
% d2(l) = data(l). MinorAxisLength;

if(1> metric(l) > 0.75 && d1(l) >40)

% % %||||||||||||||||||||||||||||||||||||||||||||||||||||||||
% %
% % %identifies the interfase level at row one and levels it to this high
% %
% % % posx(l)=data(l).Centroid(1) % extracting the drop x position
% % % leveling = posx(l) - (data(l).MajorAxisLength/2) - 20
% % % leveling = floor(posx(l) - 70 - 20)
% % leveling = floor(xcoord - 80)

```

```

% %
% %
% % L=find(finalImg_new(:,1)== 1);
% % finalImg_new2=finalImg_new;
% % finalImg_new2(L(leveling):end,:) = 1;
% %
% % figure(12)
% % subplot(1,2,2)
% % spy(finalImg_new2);
% %
% % % |||
% output.Centroid=data(1).Centroid;
% output.Area=data(1).Area;
% output.FilledArea=data(1).FilledArea;
% output.MajorAxisLength=data(1).MajorAxisLength;
% output.MinorAxisLength=data(1).MinorAxisLength;
% output.EquivDiameter=data(1).EquivDiameter;
% output.Perimeter=data(1).Perimeter;
% output.Area=data(1).Area;
% output.Area=data(1).Area;

output=data(1);
output.Roundness=metric(1);
output.FileName=filename;
output.timeFrame=timeFrame;
end
end
end
end

```